CHALMERS
UNIVERSITY OF TECHNOLOGY

Development of a criteria for squeal noise detection applicable to on-board noise monitoring

A study to evaluate existing detection methods and to seek improvements or alternatives

Master's thesis in the Master's Programme Sound and Vibration

Jesper Lennartsson
Axel Vedin

Department of Architecture and Civil Engineering
CHALMERS UNIVERSITY OF TECHNOLOGY
Gothenburg, Sweden 2024

Master's thesis ACEX30

Master's thesis ACEX30

Development of a criteria for squeal noise detection applicable to on-board noise monitoring

A study to evaluate existing detection methods and to seek improvements or alternatives

JESPER LENNARTSSON
AXEL VEDIN

CHALMERS
UNIVERSITY OF TECHNOLOGY

Department of Architecture and Civil Engineering
Division of Applied Acoustics
Vibroacoustics Group
Chalmers University of Technology
Gothenburg, Sweden 2024

Development of a criteria for squeal noise detection applicable to on-board noise monitoring
A study to evaluate existing detection methods and to seek improvements or alternatives

JESPER LENNARTSSON
AXEL VEDIN

Supervisor: Peter Torstersson, VTI
Examiner: Astrid Pieringer, Applied Acoustics

Department of Architecture and Civil Engineering
Division of Applied Acoustics
Vibroacoustics group
Chalmers University of Technology
SE-412 96 Gothenburg
Telephone +46 31 772 1000

Cover: A C30 metro train of SL (Storstockholms Lokaltrafik) at Stockholm, Sweden, photo by Region Stockholm, 2021.

Department of Architecture and Civil Engineering
Gothenburg, Sweden 2024

Development of a criteria for squeal noise detection applicable to on-board noise monitoring
A study to evaluate existing detection methods and to seek improvements or alternatives

Jesper Lennartsson
Axel Vedin
Department of Some Architecture and Civil Engineering
Division of Applied Acoustics
Vibroacoustics Group
Chalmers University of Technology

Abstract

Railway vehicles may generate a high tonal noise commonly referred to as curve squeal during navigation through curves. Typically, this noise is characterized by a single high pitch frequency accompanied by a few overtones. Its tonal character makes it more irritating for a listener than a broad-band noise at the same sound pressure level. This is a contributing factor to why curve squeal is perceived as being so disturbing.

Curve squeal is produced as a result of self-excited wheel vibrations which are triggered by large magnitude lateral forces developed in the contact between the inner wheel and the low rail. Another type of squeal noise is called flange squeal which instead originates from the outer wheel. In comparison to the tonal curve squeal, flange squeal has a more broadband character.

This study is based on noise data recorded by an onboard monitoring system during one month of traffic on the Green line of the Stockholm metro. Five different methods of detecting curve and flange squeal are evaluated. The methods accounted for are: (A) an implementation of the algorithm for curve squeal detection in operation at the Stockholm metro today, (B) an algorithm taken from literature developed by a research group at the university of Wollongong, Australia, (C) the application of a tonality module available in the commercial software ArtemiS SUITE, (D) a method devised by the authors. Finally, (E) a Hybrid method that combines method A and B. Method A is based on the sound pressure level difference between outer and inner wheels while B evaluates the spectrum of the inner wheel and looks for the highest 1/24 octave band to compare against a set criterion. C calculates the tonality of the inner wheel and marks when it is above a set limit. D calculates the sound pressure level and compares it against a threshold. All methods except C are implemented in Matlab whereas the software Artemis SUITE is used to evaluate method C.

The results showed that most of the methods did not produce accurate results rather containing many false positives.

Method A performed best with respect to curve squeal detection whereas the so-called Hybrid algorithm, containing criteria from both methods A and B, showed best abilities to detect flange squeal.

Keywords: Squeal noise, curve squeal, flange squeal, detection algorithms.

Acknowledgements

This project is carried out in collaboration between Chalmers University of Technology, the Swedish National Road and Transport Research Institute (VTI) and Tyréns Solutions AB. The ArtemiS SUITE measurements were enabled by resources funded by the HEAD Genuit Foundation under the agreement P-22/01-W. We would like to thank Astrid Pieringer from Chalmers University of Technology who has been our supervisor and examiner, Martin Höjer from Tyréns who provided us with data and support. Finally, we would like to give a big thank you to Peter Torstensson of VTI who has been our supervisor during this study and have provided help and support throughout the project, much to the benefit of both the project and our personal growth.

Jesper Lennartsson & Axel Vedin, Gothenburg, 2024

Contents

List of Figures

List of Tables

1
Introduction

Everyone who has ever been on a rail vehicle has probably experienced the unpleasant high tonal noise phenomenon called squeal noise. The noise can occur when a rail vehicle runs through a tight curve and is therefore often referred to as curve squeal. This type of noise is often regarded as the most annoying noise created by railway traffic. Thus, finding ways to identify where and why it occurs so that it may be dealt with is an important step in creating a more pleasant experience for the passengers and people in the area around rail infrastructure. The importance of this is further underlined by the fact that much rail infrastructure is located in densely populated areas where a large number of people is affected every time squeal noise is generated.

A study performed by the International Union of Railways, UIC, found that 12 % of people living within 250 m from curved tracks, who are already exposed to rolling noise above 60 dB (L_{den}), are in addition exposed to curve squeal with noise levels surpassing 80 dB. Furthermore, at the railway stations roughly 7 % of all passengers are exposed to squeal noise [1].

1.1 The structure of the study

The study is divided into three parts: Theory, Method and Results.

The Theory chapter presents a literature study giving the necessary background information on curve squeal and flanging noise. The literature reviewed covers mechanisms, origin, and features of the two types of squeal noise as well as a description of methods for detection. The Method chapter gives information on how data were obtained and analyzed. Finally, the Results chapter presents and discusses the outcome of the investigation.

1.2 Limitations

The report is based on data provided by the Stockholm metro and the consultancy firm Tyréns Solutions AB. Sound pressure signals collected by an on-board monitoring system were obtained from two metro vehicles trafficking the Green line at the Stockholm metro over the span of one month. No additional noise data were collected.

2
Theory

This chapter presents a literature review. It covers a multitude of aspects such as curving of rail vehicles and general information on squeal noise generation as well as a compilation of field studies found in literature. Three different methods for curve squeal detection found in the literature are presented. Additionally, methods for detection of impulsivity and tonality are described.

2.1 Curving of rail vehicles

Squeal noise is a result of the wheel–rail interaction during curving of rail vehicles. A railway wheelset consists of two wheels connected by a rigid axle. In curves, the inertia of the wheelset makes it move towards the outer rail. As a result, the outer wheel needs to travel a longer distance compared to the inner wheel. This is enabled by the conical wheel profile that results in a rolling radius difference as the wheelset displaces outwards in the curve. Figure 2.1 shows a schematic image of the wheel and rail contact surfaces.

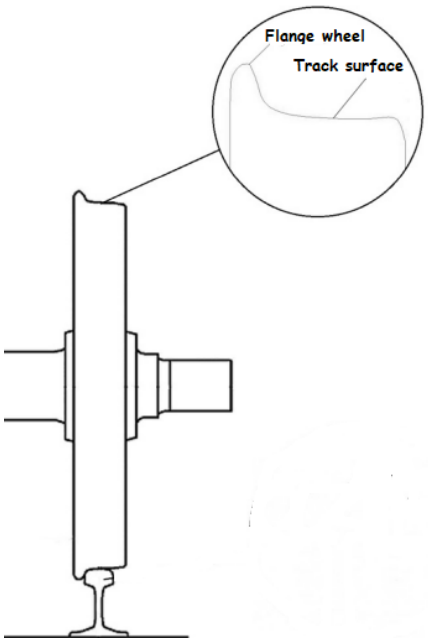

Figure 2.1: Wheel and rail contact surface. Image: Thompson [2]

This steering capacity of wheelsets are counteracted by them being mounted inside a bogie frame [2]. This arrangement is to ensure running stability at high vehicle

speeds. For passenger vehicles, the bogie provides traction and braking ability as well as support for the weight of the cars. In addition, the primary and secondary suspension of the bogie provides shock absorption. Figure 2.2 shows a typical tramcar bogie.

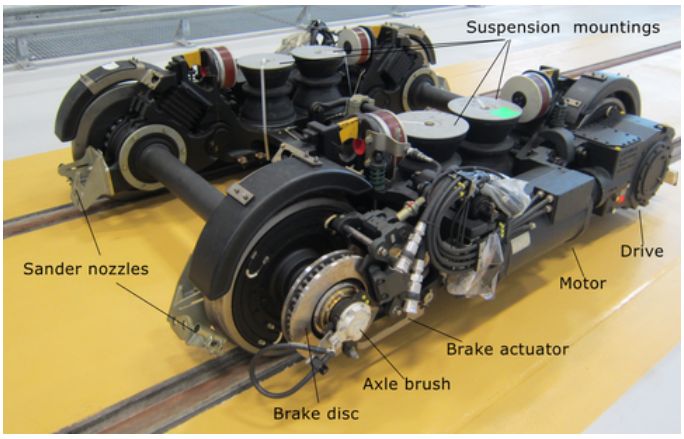

Figure 2.2: A tramcar bogie with its associated components. Image: The Railway Technical Website [3]

The train speed, curve radius, wheel and rail transverse profiles, properties of the bogie primary suspension and the inclination of the track are main characteristics of how the bogie behaves in a curve. Figure 2.3 illustrates how the leading wheelset displaces towards the outer rail during navigation through tight curves. The trailing wheelset displaces outwards towards the outer rail for increasing speed and curve radius [2], see Figure 2.4. Therefore, the angle of attack, which is the angle formed between the wheel flange and the rail when the train enters a curve, of the first wheelset is greatest for low vehicle speeds and short curve radii [2]. Due to the large angle of attack of the leading wheelset, a relative lateral velocity is created in the wheelrail contacts. The relative velocity of the wheel and rail at the point of contact normalized by the vehicle velocity is defined as creepage [2]. As soon as relative sliding, or creepage, is created, frictional wheel–rail forces also develop.

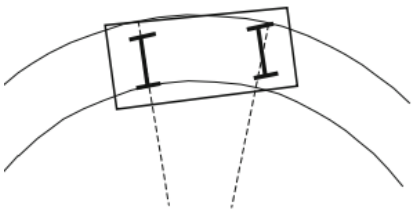

Figure 2.3: Bogie in a small curve radius with low speed. Image: Thompson [2]

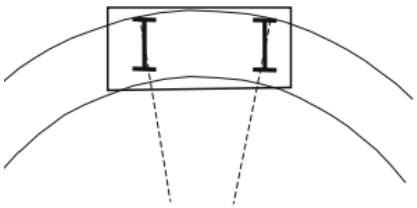

Figure 2.4: Bogie in a large curve radius with high speed. Image: Thompson [2]

Figure 2.5 shows typical contact situation at the outer and inner rail of a leading wheelset in a tight curve. The wheel–rail frictional, or creep, forces are outlined as

F2 in lateral and F1 in longitudinal direction [2]. Curve squeal is a result of the large magnitude lateral creep force developed at the inner rail.

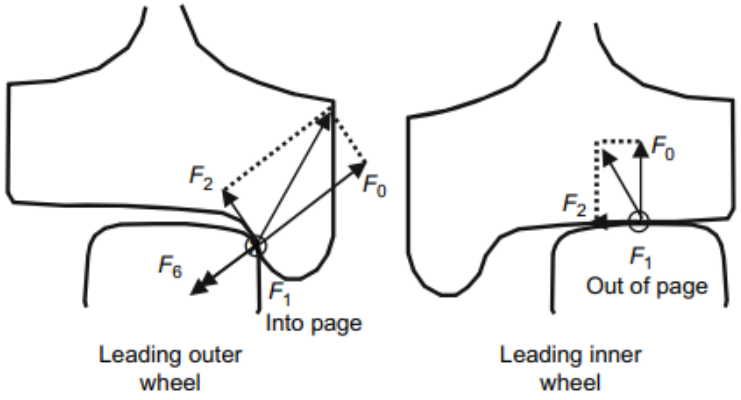

Figure 2.5: Forces acting on the wheels in a curve. F1 is the longitudinal creep force, F2 is the lateral creep force, F0 is the normal load and F6 is the spin moment. Image: Thompson [2]

2.2 What is curve squeal?

Curve squeal has a strong tonality and is generally dominated by a single high pitch frequency. An important reason why curve squeal is considered so disturbing is its tonal characteristic that makes it more annoying than a broadband noise at the same sound pressure level [2].

Curve squeal occurrence has an inverse relationship with the curve radius. A smaller radius means a larger risk for curve squeal. These short radius curves are more common in urban areas, where the number of exposed people is the greatest. This is further underlined by Rudd [4], who states as a generalization that if the curve radius R is larger than 100 times b, where b is the bogie wheelbase, no squeal will occur. The wheelbase refers to the distance between the front and rear wheelset in the bogie of a vehicle. For instance, a bogie with a 2.5 m wheelbase would not generate squeal on curves with a radius of more than 250 m, whereas a two-axle wagon with a 10 m wheelbase might be anticipated to squeal on curves up to 1000 m radius. In reality, squeal is largely absent in curves with a radius of more than about 500 m [2] and occasionally occurs in curves with radius of less than about 500 m but above 200 m. It is however widespread in curves with a radius of 200 m or less [2].

Curve squeal is radiated by self-exited wheel vibrations excited by large magnitude lateral wheelrail contact forces. The frequencies generated correspond to axial modes of the wheel and are usually in the range between 250 Hz to 5000 Hz [2], and generally above 1500 Hz [5] but may also appear at higher frequencies. As for flanging squeal noise, it is the contact between the flange of the wheel and the gauge face of the rail that generates this type of noise. Flanging squeal noise may occur across the

spectrum and is characterized by a broadband frequency spectrum rather than a highly tonal spectrum [6]. Additionally, it is usually not as loud as curve squeal [5].

Due to the anatomy of the human ear, human hearing is most sensitive in the frequency range between 1000 Hz and 5000 Hz. This coincides with the frequency region where curve squeal is mostly generated and hence are perceived as relatively louder. Equal loudness contours were developed to establish the relationship between frequency and perceived loudness. One of the earlier versions was developed by Fletcher and Munson in 1933 and labeled Fletcher–Munson curves [7]. Since loudness is subjective, the curves were compiled from the results of listening tests. In the tests, the strength of signals of different frequencies was adjusted until the participants experienced it to be of equal loudness as a reference signal at 1000 Hz. These curves have since been updated, with ISO 226 [8] being the current standard. The Equal loudness curves from the ISO standard are highlighted in Figure 2.6. Loudness level is measured in phon. Phon and decibel line up at 1000 Hz, where a 50 dB signal would be equivalent in loudness level to 50 phon, while, for other frequencies they differ, as seen in Figure 2.6.

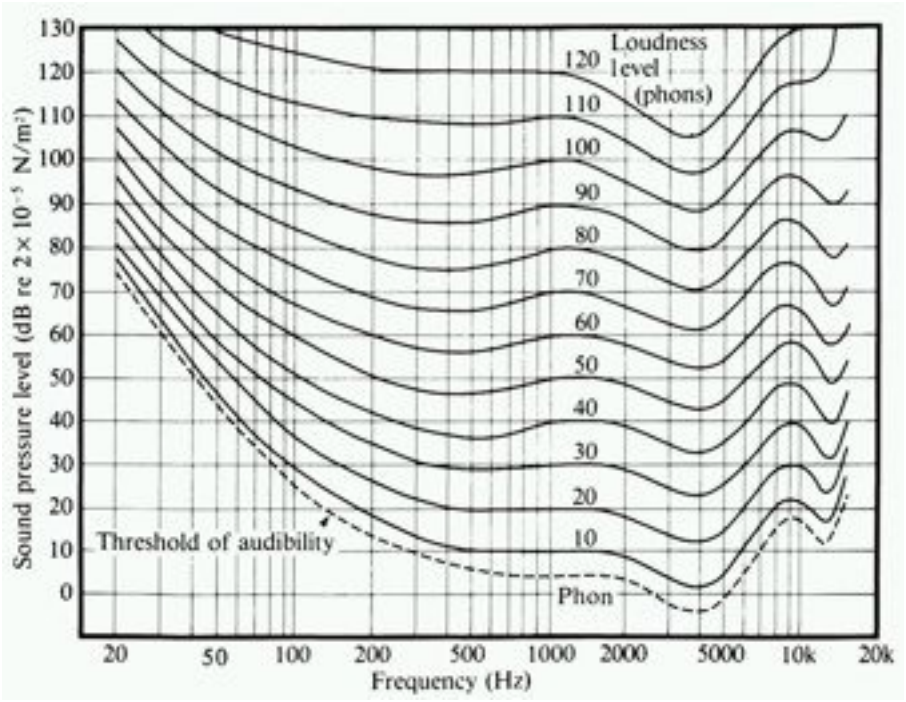

Figure 2.6: Equal Loudness Contour, ISO 226:2003 [8]

2.3 Field observations of squeal noise

A distinction is made between curve squeal and flange squeal. Figure 2.7 shows the spectrogram for a curve passage containing curve squeal. As seen in the figure, curve squeal has a strong tonality, dominated by a few narrow bands, as previously mentioned generally above 1.5 kHz, and at a sound pressure level above the rolling noise level. The curve squeal event illustrated in Figure 2.7 is based on data collected by the Quiet Track Monitoring System (QTMS), which is described more in detail in the subsequent Section 3.1. The passage in the figure is identified by a twelve-digit numerical label.

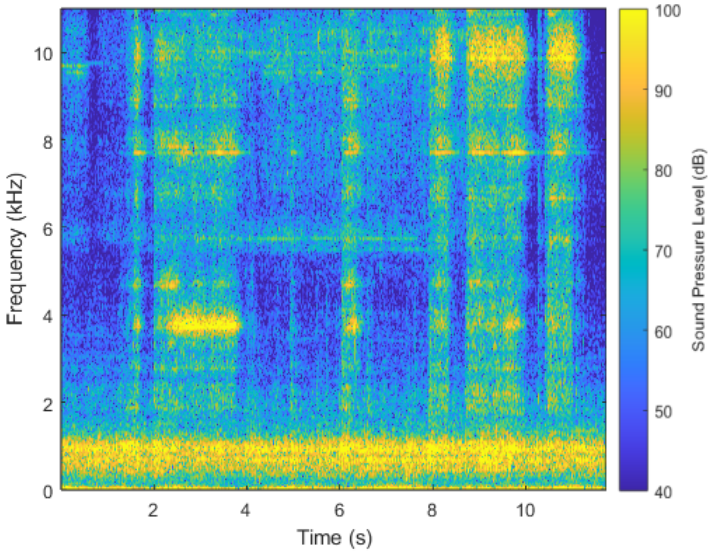

Figure 2.7: Spectrogram showing a suspected curve squeal event. Data from QTMS, passage identifier 738440335064, curve radius 214 m.

Table 2.1 summarizes field studies on curve squeal noise found in literature. Selected few key aspects, such as curve radius, vehicle speed and squeal frequencies are outlined. As is clearly discernible from the table, squeal noise covers a wide range of frequencies, from 400 Hz up to 8000 Hz.

Table 2.1: Summery of field studies on curve squeal found in literature.

Radius (m)	Speed (km/h)	Frequency (Hz)	Vehicle type	Location	Reference
17.5	n/a	1500	Tram	Milan, Italy	Corradi et al. [9]
25	5	800	Tram	Victoria, Spain	Merideno et al. [10]
60	10-40	400-8100	Tram	Grenoble, France	Vincent et al. [11]
n/a	n/a	500, 1250, 1600	Tram	Netherlands	Van Ruiten [12]
75	10-40	450-6200	Suburban	Paris, France	Vincent et al. [11]
180	n/a	800, 1200, 2300, 4000	Suburban	n/a	Unpublished reference [13]
200	Low speed	4100	Suburban	Bern, Switzerland	Glocker et al. [6]
160-240	n/a	2200, 2900, 3600, 4500	Suburban	North Wales, United Kingdom	Thompson [2]
284	n/a	1000-8000	Freight	Sydney, Australia	Jiang et al. [14]
315	75	1600-2500, 4000 and above	Freight	North of Sydney, Australia	Anderson [15]
1000	50-70	3800-4800	Freight	Elands bay, South Africa	Fourie et al. [16]

Flanging squeal noise has a more broadband characteristic [5]. Even though it is also generated at a higher sound pressure level then the rolling noise, it is not as loud as curve squeal, hence it is perceived as less annoying than curve squeal [5]. Figure 2.8 shows a passage with outer wheel squeal typical for the Stockholm metro. The term "outer wheel squeal" is used instead of flanging noise as the location of the contact between the outer wheel and high rail has not been able to verify (i.e. if it is made between the wheel flange and the rail gauge face).

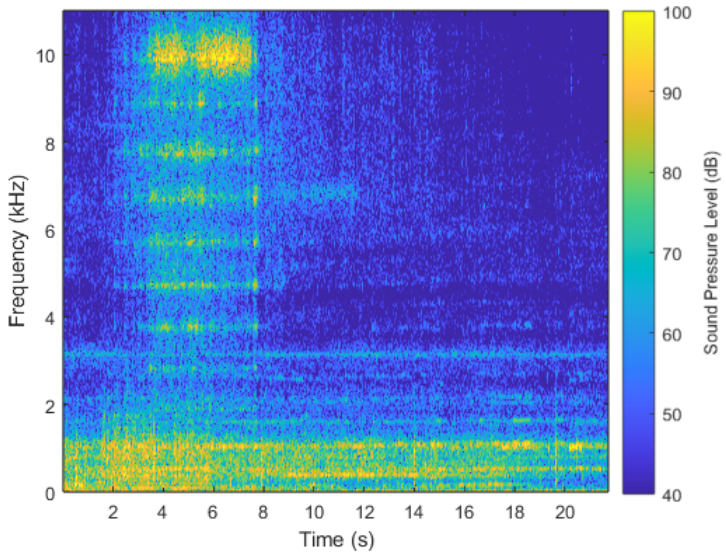

Figure 2.8: Spectrogram showing a suspected outer wheel squeal event. Data from QTMS, passage identifier 738436845454, curve radius 122 m.

Table 2.2 shows a summary of field studies on flange squeal. As for Table 2.1, selected few key aspects, such as radius, vehicle speed and squeal frequencies are outlined. In contrast to curve squeal, flange squeal covers a wide range of frequencies, from 1 kHz up to 20 kHz, which significantly exceeds the limit for curve squeal.

Table 2.2: Summary of field studies on flange squeal found in literature.

Radius (m)	Speed (km/h)	Frequency (Hz)	Vehicle type	Location	Reference
150	5, 20, 25, 30	1000 - 10 000	EMU	South Korea	Kim et al. [17]
200	n/a	1600 - 10 000	Metro	Högdalen, Sweden	Nilsson et al. [18]
200	Low speed	2000 - 13 000	Suburban	Bern, Switzerland	Glocker et al. [6]
1000	80, 110	2000 - 20 000	Metro	Hongkong	Lou et al. [19]

2.4 Noise characteristics

Noise is defined as unwanted sound. Curve squeal has two main characteristics: tonality and impulsivity. Both add to the annoyance experienced by a listener. In the following two subsections, tonality and impulsivity are described.

2.4.1 Tonality

Sounds are made up from either pure tones or a combination of many different tones. In case of the latter, the sound can be referred to as complex. A pure tone sound consists of a single frequency, such a sound is produced by a tuning fork or a whistle. A complex sound may be dominated by a specific tone or a narrow band. In these cases the sound is characterized as tonal and perceived as a tone rather than as a complex sound [20].

Tonality is a way to describe the relative weight of the tonal components in each noise spectrum [20]. Tonality can be measured in different ways. Tone-to-noise ratio and prominence ratio are two different methods described in the ECMA-418 [21] standard. This, in turn, is in accordance with the ECMA-74 [22] standard. Another method is described in the standard DIN 45681 [23] or ISO/TS 20065:2022 [24]. The latter is based on the former. A short overview of these different methods is found below.

In 2019, Sottek and Becker conducted a study about the frequency-dependent differences between equal-tonal-loudness contours and equal-tonal-annoyance contours [25]. In the study, a listening experiment was conducted using the so-called adaptive two-alternative forced-choice method, which is a method were the participants are forced to choose between two preselected options when asked about their response to stimulus, an example would be "top or bottom" when asked where on a screen a dim light flashed. This adaptive approach efficiently determines perceptual thresholds for tonal loudness and annoyance. The participants were a group of 20 people ages between 23 and 40 years with normal hearing. The result of the experiment with regards to the equal annoyance and the equal loudness can be seen in Figure 2.9. A close relationship between the perception of annoyance of tonal sounds and the perception of loudness for frequencies under 1000 Hz is found. However, for higher frequencies the annoyance for tonal sounds increases. In Figure 2.9 this is seen by the equal annoyance curve decreasing as the frequency is increased. The equal annoyance curve has a sharp decrease for frequencies above 1000 Hz illustrating that sound at these low levels is perceived as equally annoying to higher sound pressure levels in the low frequency range.

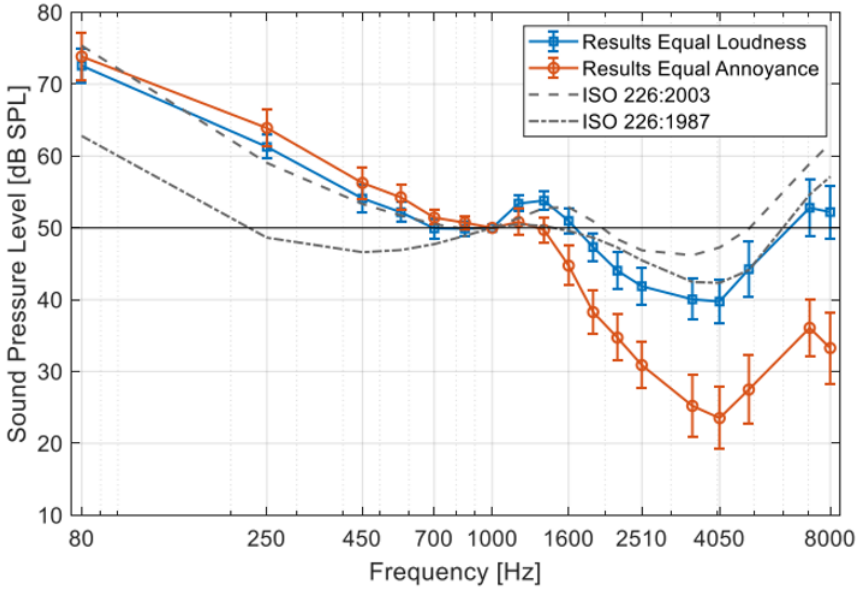

Figure 2.9: Correlation between sound pressure level and frequency for equal loudness and equal annoyance contours. Image: Sottek [25]

2.4.1.1 Tone-to-Noise Ratio

To evaluate the Tone-to-noise ratio, the first step is to perform a Fast Fourier Transform (FFT) analysis on the raw signal. Thereafter, levels of discrete tones are determined by calculating the sound pressure level for narrow frequency bands that contain the identified tonal frequency component. When the sound pressure level of the tone is obtained, the level of the masking noise is determined using critical bands.

Critical bands, first introduced by Fletcher in 1933 [7] are used to quantify the ability of the human ear to distinguish between individual frequency tones [26]. These bands are based on how the cochlea, the hearing organ within the inner ear, reacts to sound. Different parts of the cochlea are excited by different frequencies ranges. These ranges correspond to the critical bands.

The width of a critical band depends on the frequency of the sound. At low frequencies, critical bands are narrower and as the frequencies increase the bands gets wider. As a result, differentiating between two tones at a higher frequency is harder than differentiating two tones, with the same difference, at a lower frequency.

The level of a critical band refer to the energy distribution within individual critical bands and can be derived from the spectral energy distribution of a sound, where the energy within each critical band is summed up to determine the overall level within that band.

When one has both the tone level and masking noise level, the Tone-to-noise ratio is calculated as the difference between the two, expressed in dB. For frequencies above 1000 Hz the tone is classified as prominent, meaning clearly audible, if the Tone-to-noise ratio is 8 dB or higher. An example of a prominent tone can be seen in Figure 2.10.

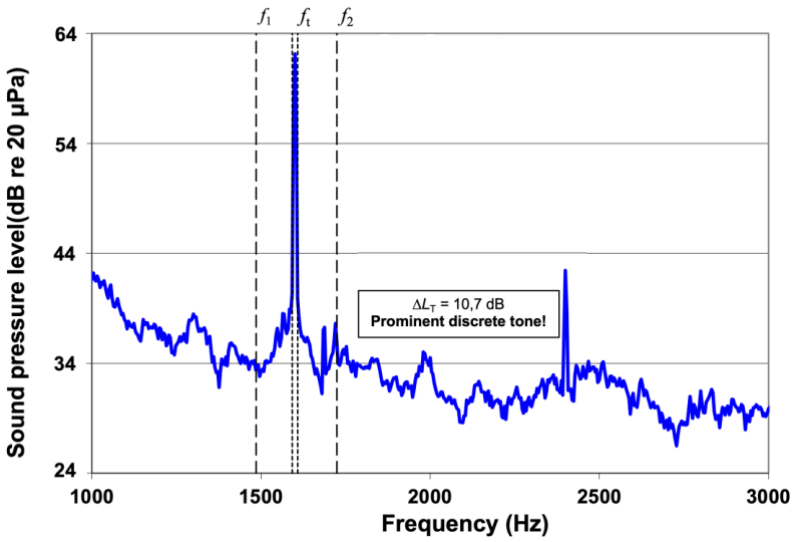

Figure 2.10: An example of a prominent tone detected by Tone-to-Noise ratio. Image: ENCA-418 [21]

2.4.1.2 Prominence Ratio

The Prominence ratio is evaluated by first performing a Fast Fourier transform of the raw signal to acquire either the spectral density or sound pressure level spectral components. Thereafter the levels of the critical bands are determined, see Section 2.4.1.1. The calculation of the Prominence differs slightly depending on if the frequency is above or below 171.4 Hz. For frequencies above 1000 Hz, a tone is classified as prominent if the level of the critical band is 9 dB or more above the neighboring bands. An example of a prominent tone can be seen in Figure 2.11. For frequencies below 1000 Hz, the critical band level L_T must be larger than the threshold given by Equation 2.1 in order to be classified as prominence.

$$L_T > 8 + 8,3 * lg(\frac{1000}{f}) \tag{2.1}$$

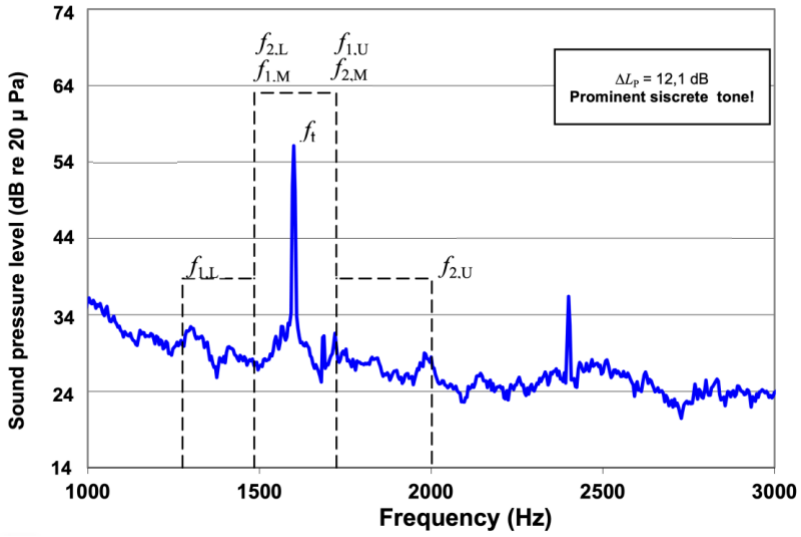

Figure 2.11: An example of a prominent tone detected by Prominence ratio. Image: ENCA-418 [21]

2.4.1.3 ISO 20065 method

The ISO 20065 [27] standard covers a method for assessing the audibility of a tone in noise. The method uses an A-weighted signal and begins by determining the width of the critical band, followed by a determination of prominent tones and the mean narrowband. A narrowband signal is one that is concentrated within a small range of frequencies. Following the determination of the narrowband, the tone level is calculated. Thereafter, the distinctness of the tone, which is a measurement on how easily a distinguished from other tones, which depends on the bandwidth of the tone and its edge steepness, a measurement on how rapidly the amplitude of a sound wave changes at the onset or offset of a sound is obtained. The penultimate step is determining the narrowband level of the masking noise in the critical band. The audibility of the tone can then be calculated as the difference between tone level and masking threshold.

2.4.2 Impulsivity

According to the Center for Disease Control and Prevention, impulsivity is defined as the instantaneous change in sound pressure over a short amount of time [28]. An example of an impulsive sound would be that of a gunshot or a sledgehammer blow. Compared to continuous noise, impulsive noise is more likely to cause hearing loss as exposure to high-intensity impulses can lead to mechanical damage to the inner ear as well as acoustic trauma. Curve squeal is unlikely to cause this kind of damages even if it is impulsive, e.g. Figure 2.7, but as stated earlier the impulsivity adds to the level of annoyance of the noise.

This is further underscored by the Nordtest method NT ACOU 112 where an adjustment, a penalty, is applied to the measurement if prominent impulses are present

[29]. This accounts for the increased annoyance perceived for impulses with high audibility, or perceived prominence. The method uses an A-weighted sound pressure level time profile with fast time weighting. The predicted prominence depends on the onset rate of the impulse, which is a positive proportional increase in sound pressure level caused be the impulse in dB/s, and in addition the predicted prominence which also depends on the magnitude of the impulse.

Rajala and Hongisto [30] investigated if impulsive noise is being perceived as more annoying than steady-state noise. A psychoacoustic experiment with a group of 74 participants aged between 20 to 44 years were performed. The participants were exposed to an impulsive sound as well as a reference, continuous, sound. A variation of impulsive sounds at different levels (D_L) and onset rates (R_{on}) were used. Results for two different sounds can be seen in Figure 2.12. Impulsive sounds with a level difference of 10 dB or more are noticed to be more annoying than continuous sound.

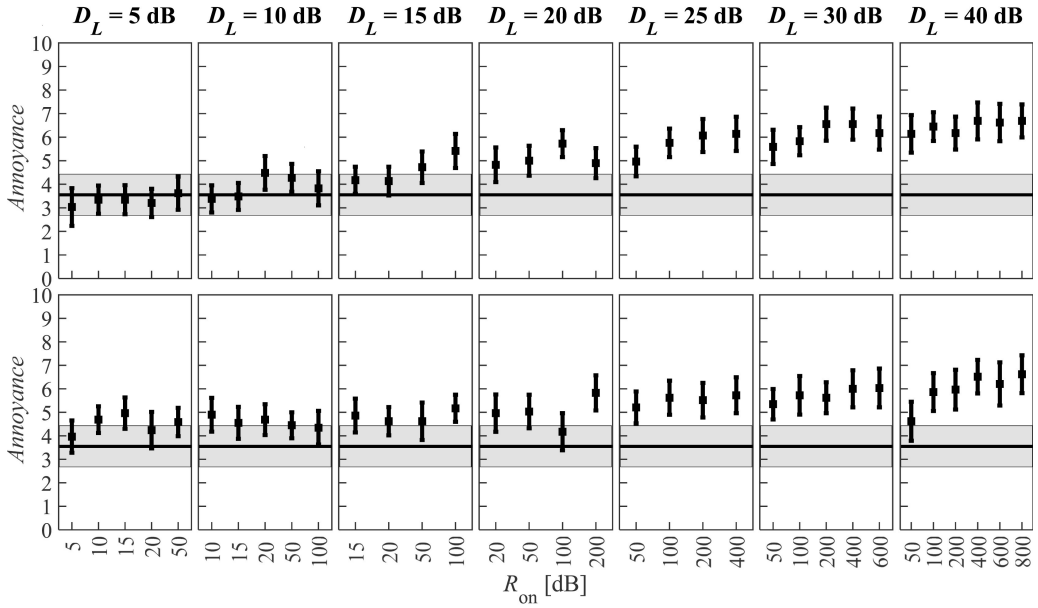

Figure 2.12: Resulting annoyance for two different sounds, of varying sound pressure levels and onset rates. The upper row show the first signal and the lower panels the second signal. The grey area shows annoyance range for non-impulse sound while the black vertical lines the annoyance for the impulse sound. Image: Rajala [30]

In another paper it is found that impulsive sound causes higher stress levels and lower performance than continuous sound [31]. The studied group consisted of 59 people in ages ranging from 20 to 42 years. The group was exposed to impulsive sound at 65 dB while performing tasks requiring constant concentration. Two reference sounds were used corresponding to a continuous sound at 65 dB, as well as a quieter sound at 35 dB. Figure 2.13 shows the difference in annoyance perceived by the participants. The impulsive sound was found to generate the most annoyance.

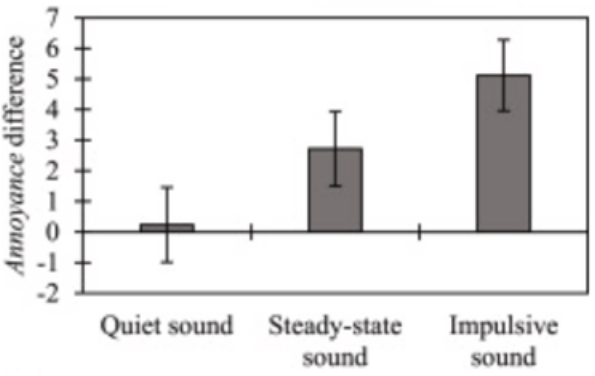

Figure 2.13: Difference in annoyance between quiet, steady-state and impulsive sound. Image: Radun [31]

2.5 Squeal noise detection

This section describes different methods to detect curve squeal found in literature.

2.5.1 Stockholm Algorithm

The Stockholm algorithm, below referred to as method A, corresponds to the algorithm used in the Stockholm subway to detect curve squeal as part of the Quiet Track Monitoring System developed by the company Tyréns. More details about the monitoring system is found in Section 3.1. Details on this method have been provided in private communication with Peter Torstensson, VTI, the 25th of January 2023. The method requires noise recorded simultaneously from the outer and inner wheel–rail contact. First both signals are A-weighted and band-pass filtered in the frequency range between 1600 Hz to 6300 Hz. This removes the low frequency rolling noise. Next the level difference between the outer and inner wheel is evaluated at sampling frequency of 4 Hz. A squeal event is defined as a case when the level evaluated for the inner wheel exceeds that of the outer wheel by at least 3 dB while simultaneously having an absolute level above 95 dB.

2.5.2 Wollongong Algorithm

The Wollongong algorithm, referred to as method B below, is derived from literature and corresponds to an algorithm developed at the university of Wollongong, Australia, to detect curve squeal and flanging noise based on wayside measurements [32]. The method uses a fast weighting 1/24-octave spectrum continuously evaluated during the passage through a curve.

Squeal is detected if one band in the frequency range between 1 kHz to 10 kHz fulfills both of the following criteria:

1. It has the highest-level spectral component within the spectrum, and
2. The level is greater than the neighboring bands by at least 10 dB.

For flanging noise, a separate detection method is used based on an energy ratio between the energy inside the bounds of 2 kHz to 10 kHz, not counting any squeal noise found, and the total energy in the spectrum. A ratio above 0.8 is considered as flanging noise.

2.5.3 SoundScience Algorithm

Another algorithm for squeal noise detection is designed by SoundScience (SS), Australia [32]. It focuses on the detection of tonal noise components and does not currently support flange squeal detection. In comparison to the Wollongong algorithm, the SS algorithm is able to detect lower-level and less obvious tones. It may also detect multiple simultaneous tones [32].

The methodology used is more complex than the Wollongong algorithm. It uses a modified Canny edge detection algorithm [33], which is applied to a spectrogram. A Canny edge detector is an edge detection technique that detects edges in an images. Using the detected edges, structural information is extracted.

An explanation of the procedure is as follows: (1) A spectrogram is obtained by performing a short-term Fast Fourier Transformation, (2) contrast values for bins that make up the spectrogram are calculated and bins with high values are merged into lines and (3) lines are checked and those with frequencies reaching values between 1 kHz and 10 kHz for a minimum of one second are marked as squeal.

2.5.4 ArtemiS SUITE

ArtemiS SUITE, below referred to as method C, is a software for measuring and analyzing sound and vibrations developed by Head Acoustics. In this study, the software is used to calculate the tonality of the signal obtained from measurements of vehicle passages. This is done by running a built-in analysis tool called *Tonality (hearing Model) vs. Time*. This tool is based on the ECMA-418-2 standard, see Section 2.4, and calculates the tonality values over time using 16 bits per sample. The data is then screened to find tonal events in noise recorded from vehicle passages. According to ECMA-418, the signal is considered tonal, if the tonality value is greater than 0.4 T/tuHMS [34]. Where T/tuHMS stands for Tonality over Tonality Units according to the Hearing Model of Sottek.

2.5.5 Peak value method

While the aforementioned methods have been based on already established methods, this final method is instead derived from the literature study and will be referred to as method D going forward. As curve squeal is usually of greater strength then surrounding non-squeal sound, this method looks for peak values of the signal and determines if they fall inside the frequency range of interest. In this case, this range is 2000 Hz or higher.

The algorithm divides the signal into blocks of 1/4 second lengths and then calculates a 1/24-octave band spectrum for each block. The peak value of each block is then compared against each other to find the peak value for the entire signal. This value is then compared against a base value, which is the same as the one used in the Stockholm algorithm, 95 dB. If the peak value exceeds the base value, the passage is marked as containing squeal noise.

2.6 Condition health monitoring

Effective maintenance of railway wheels requires knowledge of their physical condition health. As a result, the collection of data is the focus of many maintenance planning procedures. Condition monitoring is defined as continuous or periodic collection, analysis, and interpretation of data to reveal the state of an object and determine whether maintenance is required [35]. The data used for this report has been obtained from a noise-based condition health monitoring system, see Section 3.1. Another example of a monitoring system called Acoustic Rail-Influence Recording is described below. Additionally, the use of Axle Box Acceleration to monitor track condition health is discussed.

Acoustic Rail-Influence Recording or ARRoW is a sound-based system that measures sound levels, position, and speed [36]. The system is used to detect rail squats. A squat is a rolling contact fatigue damage that shows as a widened imprint on the rail surface and is usually identified by a pattern of surface cracks. The system uses four microphones, one near each wheel of the four-wheel bogie, to measure the sound level close to the wheels. One can easily discern between the left and right rail due to this microphone set-up. This method has been used on the railway line between Tilburg and Den Bosch in the Netherlands. The algorithm uses three criteria to detect squats. The first criterion controls that an increase in sound level is detected on both microphones placed at the same side of the bogie. The second criterion considers that the sound level increase should be higher than a certain threshold. The third criterion ensures that if the first microphone indicate a peak in sound pressure level it should be detected a few milliseconds later at a time instant determined by the traveling speed and the distance between the two microphones. The threshold selected for use in this algorithm is the key to a successfull identification since a threshold set too low may yield false-positives results [36].

Axle Box Acceleration, or ABA for short, is a quantity often involved in procedures to monitor mechanical degradation of wheels and tracks. Information on the wheel-track structure is extracted from the measured accelerations as each track will have a specific signature. Track mechanical degradation is detectable when compared to a functioning track's signature. This means that ABA can only be used where one has recorded the signature of a healthy track. Figure 2.14 illustrates a monitoring system including accelerometers mounted at the axle box of the wheelset [37].

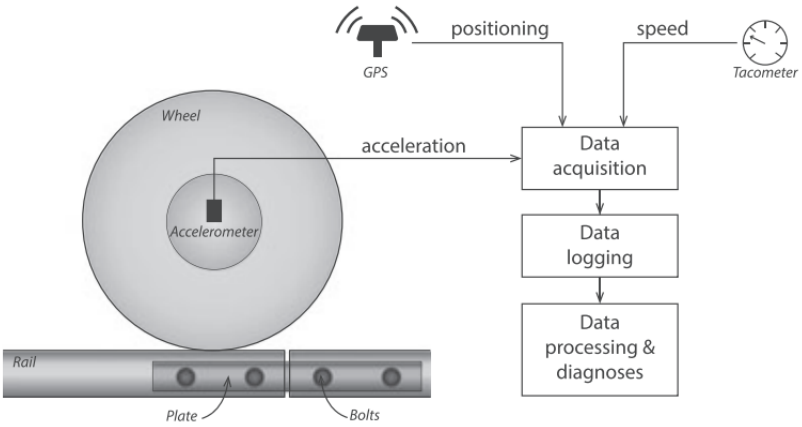

Figure 2.14: Schematic view of ABA. Image: Oregui [37]

3
Method

3.1 Track monitoring and data acquisition

As previously mentioned in Section 1.2, no measurements were performed by the authors, instead data were provided to the project by Tyréns. This data had been collected using the Quiet Track Monitoring System (QTMS) developed by Tyréns [38] and implemented on seven metro trains of type Bombardier C20 operating on the Stockholm metro. QTMS was originally developed as part of the EU-financed project *Quiet Track* [39] with the objective to enhance maintenance through use of condition health monitoring.

The QTMS is mounted on metro trains operating on three different lines (Green, Red and Blue) of the Stockholm metro, see Figure 3.1. The data used in this study are taken from the Green line.

Figure 3.1: Network map of the metro in Stockholm. Imag KTH [40]

Regarding the measurement setup, microphones are mounted behind the front bogie of the leading car or in front of the bogie of the trailing car. A C20 trainset is composed of 2-3 units of 47 m length. Each unit is a semi-trailer arrangement with one central car with two bogies, and two hinged end cars with one bogie each. P1 and P2 in Figure 3.2 indicate the microphones positions on the vehicle. At both P1 and P2 are microphones mounted at each side of the vehicle, making the installation to be composed of a total of four microphones. However, for the current study, only microphones used for the purpose to detect curve squeal located at the P1 position, are used.

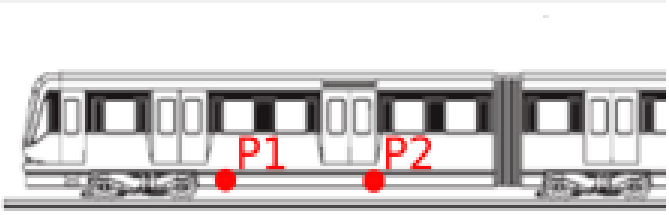

Figure 3.2: Schematic view of the C20 train, showing the locations of microphones in the QTMS. Image Vinberg [41]

3.2 Data-set information

Raw data were provided by the QTMS in the form of five minute recordings sampled at 22 kHz in the flac file format. Each file was accompanied by a text file containing metadata such as the time and date of the recording, the type of curve and its radius, if the vehicle is traveling north or south, and which channel corresponds to which wheel, as well as information on its location with respect to the inner and outer rail in the curve.

Data were obtained from a metro train in ordinary operation during October 2021 and contained a total of 3350 curve passages. The curves are divided into four categories depending on their radius. The number of passages for each of the categories as well as their corresponding radii range is found in Table 3.1.

Table 3.1: Basic information on the four curve categories.

Category	Radius [m]	Number of passages
1	101-200	431
2	201-300	854
3	301-400	1455
4	401-500	610

3.3 Implementation of squeal detection methods

This section discusses the implementation of the four methods (A, B, C and D) for squeal noise detection accounted for in the current study. For a general description of the different methods considered see Section 2.5.

Implementation of method A, B and D was performed in the software Matlab. For the evaluation of method C the commercial software Artemis SUITE was used. The implementation of method A was validated by comparison towards results from the curve squeal noise detection performed by the QTMS-system in operation at the Stockholm metro. Figure 3.3 shows an example of the good agreement between the implementation of method A performed by the authors and that in operation at the Stockholm metro.

With regards to method B, an alternative implementation were also used, where the threshold was lowered. Additionally, as Method B as an algorithm for both types of squeal noise. Both algorithms were applied for each squeal type.

In addition to methods A-C developed to detect curve squeal radiated from the inner wheel the potential to detect squeal emitted from the outer wheel has been investigated. This was performed using a procedure similar to that of method A, but instead searching for events when the filtered sound pressure level measured at the outer wheel exceeds that of the inner wheel by 3 dB.

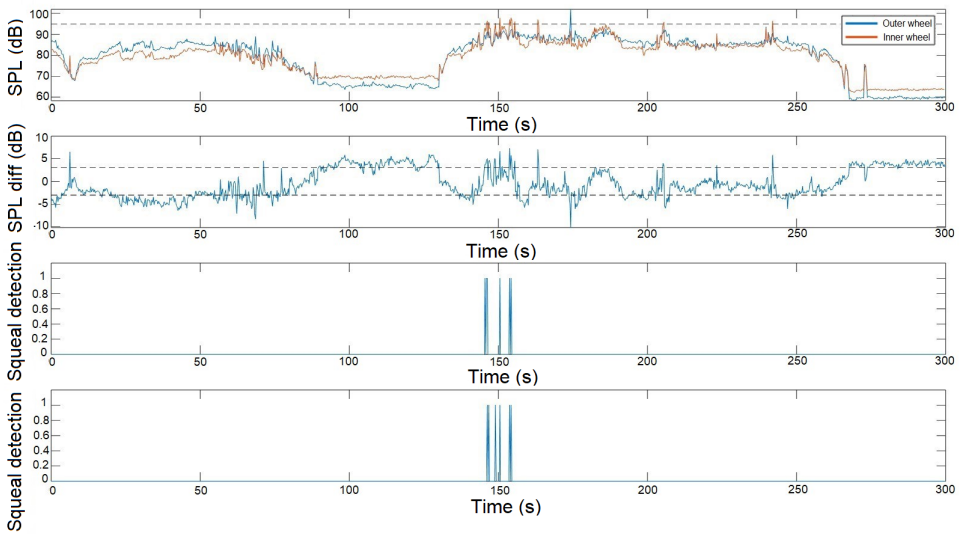

Figure 3.3: Comparison of the implementation of method A and that in operation at the Stockholm metro. For the two lower diagrams, 1 means squeal and 0 means no squeal.

3.4 Assessment of squeal detection methods

For the assessment of the methods for curve squeal detection, the results of method A is used as reference. The definition of curve squeal is in part subjective. Therefore, method A, whose abilities with respect to curve squeal detection have been verified by previous studies, was used for comparison. Additional confidence in method A was gained through listening tests and inspection of spectrograms of randomly selected vehicle passages.

In the first step of the assessment of squeal detection methods a screening is performed. Thereafter results of methods B and C are compared to those of method A by considering the following categories:

- True Positive
- True Negative
- False Positive
- False Negative

Where true positive means both methods have found squeal for the current passage. True negative means that both methods found no squeal for the current passage. A false positive means that the assessed method have found squeal for a case when method A did not. For a false negative case the assessed method did not find squeal for an occasion when method A did detect curve squeal.

For the true positive results, the total squeal time of passages is calculated. Additionally, the time instants during passages when the methods detect squeal occurrence are marked. This since the methods marks different part of the same passage for squeal, see Figure 3.4 and 3.5.

Figure 3.4 shows spectrograms for a passage where a method has detected curve squeal. The settings used for the spectrograms were; Hanning window with a length of 4096, a 50 % overlap and a FFT length of 4096. Black and magenta lines are used to indicate when the algorithms have detected squeal. The black vertical lines indicate the beginning and end of a curve squeal noise detection, respectively. Figure 3.5 show spectrogram for a vehicle passage where a method has detected outer wheel squeal.

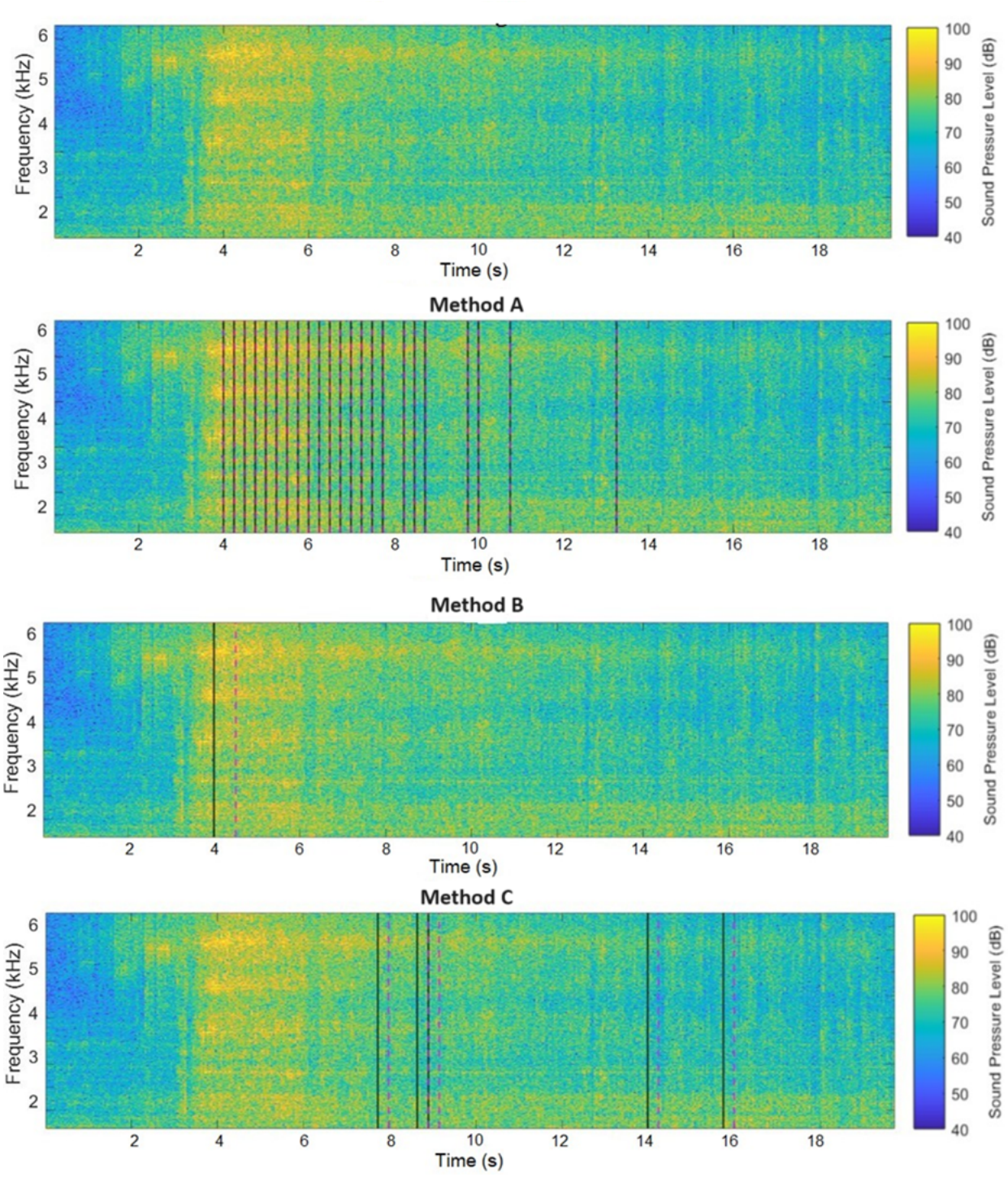

Figure 3.4: Comparison of the results of the different detection methods for the QTMS passage identifier 738456359119, curve radius 200 m.

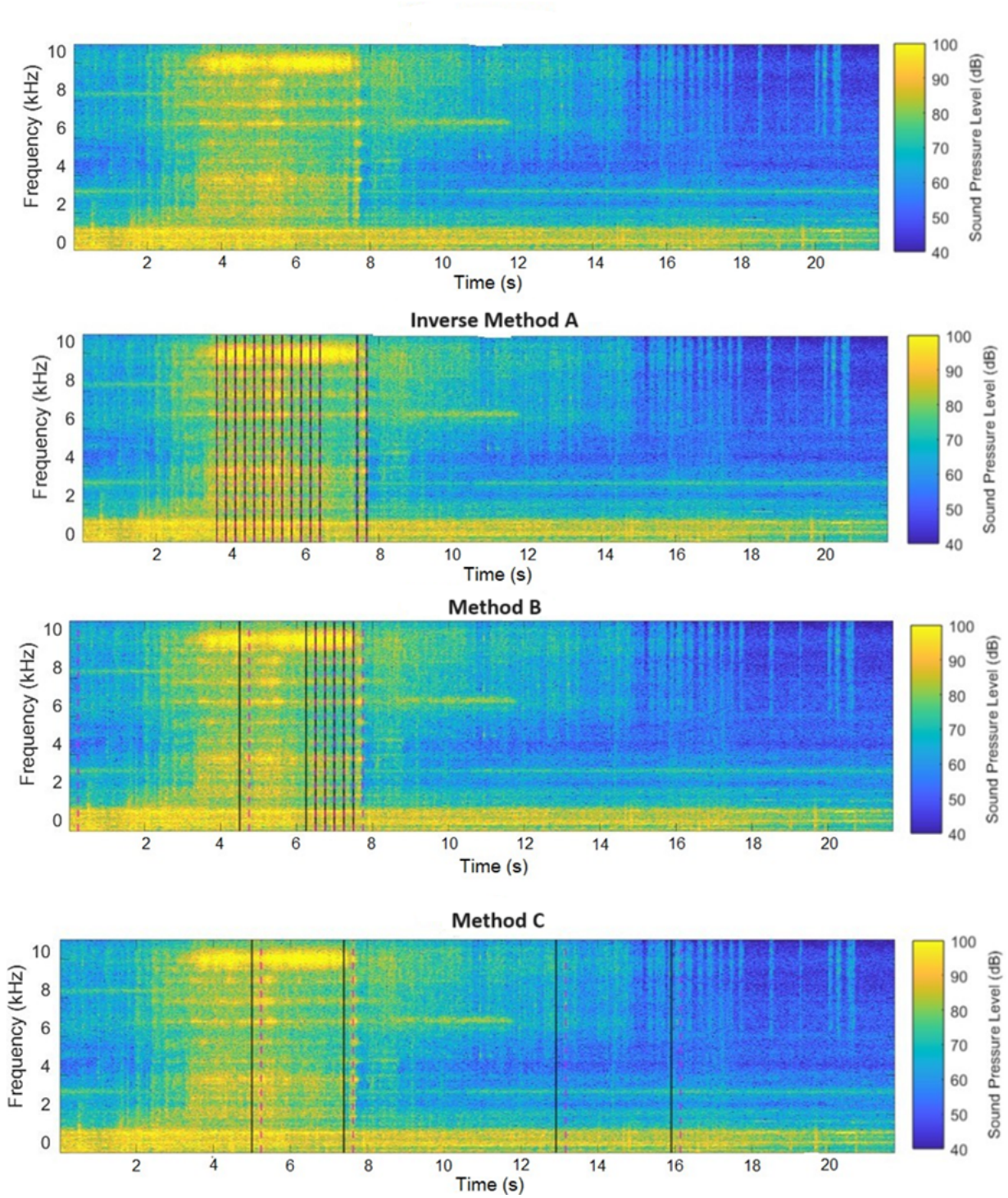

Figure 3.5: Comparison of the results of the different detection methods for the QTMS passage identifier 738436845454, curve radius 115 m.

4

Results

In this chapter, the results from the different methods used for the detection of curve squeal and outer wheel squeal on the Stockholm metro are presented and analyzed. As the number of vehicle passages exceeds 3000, only a few passages with typical characteristics for the different methods and squeal types are highlighted. As a supplement, tables containing the total number of detections are also included. In the following squeal noise detected by the microphone mounted close to the outer and inner wheel of the instrumented wheelset of the QTMS-system will be referred to outer and inner wheel squeal, respectively.

4.1 Squeal noise characteristics

Noise from curve passages recorded by QTMS during October 2019 is used to illustrate the noise characteristics for outer and inner wheel squeal. More information on QTMS is found in Section 3.1.

The two types of squeal are identified following the criteria outlined in Section 2.5. The end of the instrumented train that runs in front alternates and therefore a procedure for identifying the wheel running towards the high and low rail has been developed.

Figure 4.1 shows example spectra of outer and inner wheel squeal as well as a case without squeal for three passages through curves with similar radius. The spectra were calculated using window type Hanning and FFT-length 4096. The broadband noise content in the frequency range below 1000 Hz is noticed to be similar for the three passages. Nevertheless, a significant difference in sound pressure levels exists among the three passages, even within the frequency range predominantly characterized by rolling noise Notably, both squealing passages contain significantly higher levels compared to the passage without squeal noise. It should be noted that factors influencing the level of rolling noise such as rail roughness levels and vehicle speed are not considered as part of the current analysis. The corresponding spectrograms are presented in Figure 4.2.

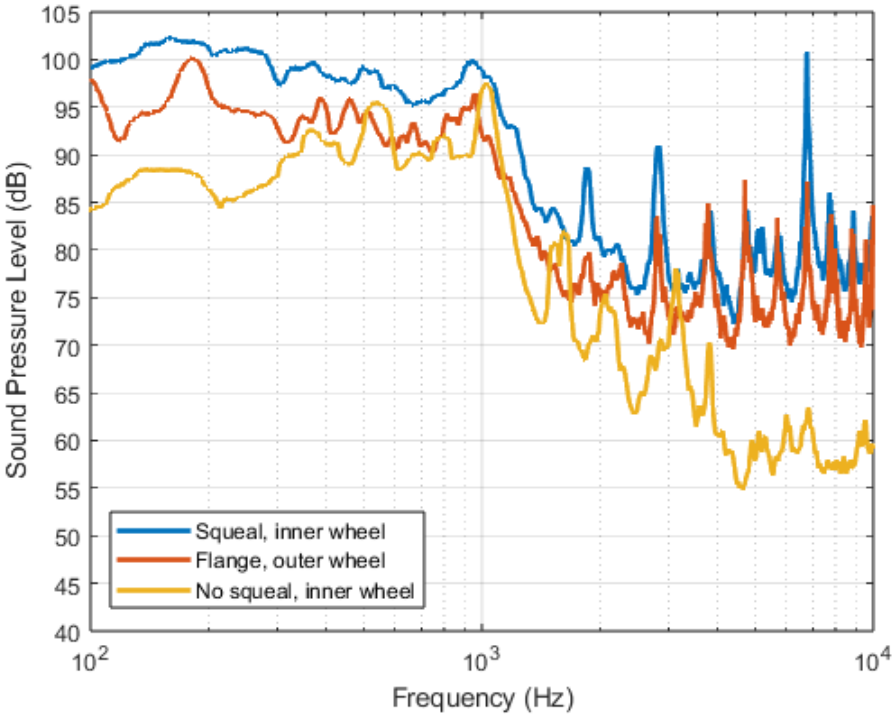

Figure 4.1: Example sound pressure level spectra for passages containing inner wheel squeal (QTMS passage identifier 738441285922, curve radius 118 m), outer wheel squeal (QTMS passage identifier 738436845454, curve radius 115) and no squeal (QTMS passage identifier 73844098784, curve radius 122 m).

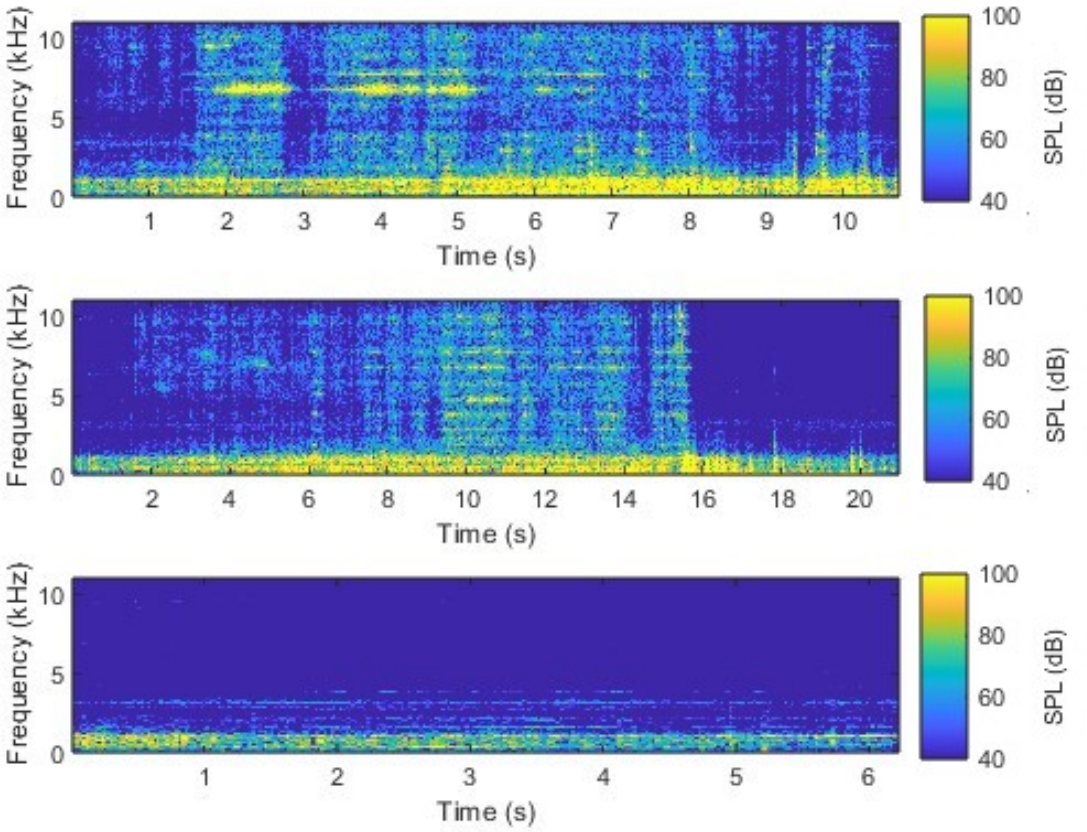

Figure 4.2: Example sound pressure level spectrograms for passages containing; Top figure: Inner wheel squeal (QTMS passage identifier 738441285922, curve radius 118 m), Middle figure: Outer wheel squeal (QTMS passage identifier 738436845454, curve radius 115) and Bottom figure: No squeal (QTMS passage identifier 73844098784, curve radius 122 m).

Figure 4.3 and Figure 4.4 show the spectra and spectrogram respectively for a curve passage with inner wheel squeal.

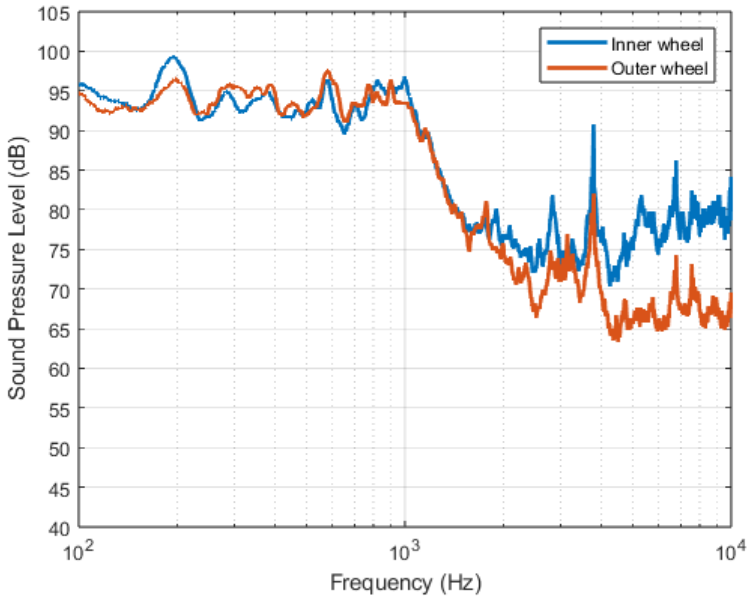

Figure 4.3: Sound pressure level spectra of an example curve passage that contains inner wheel squeal. QTMS passage identifier 738436439204, curve radius 178 m.

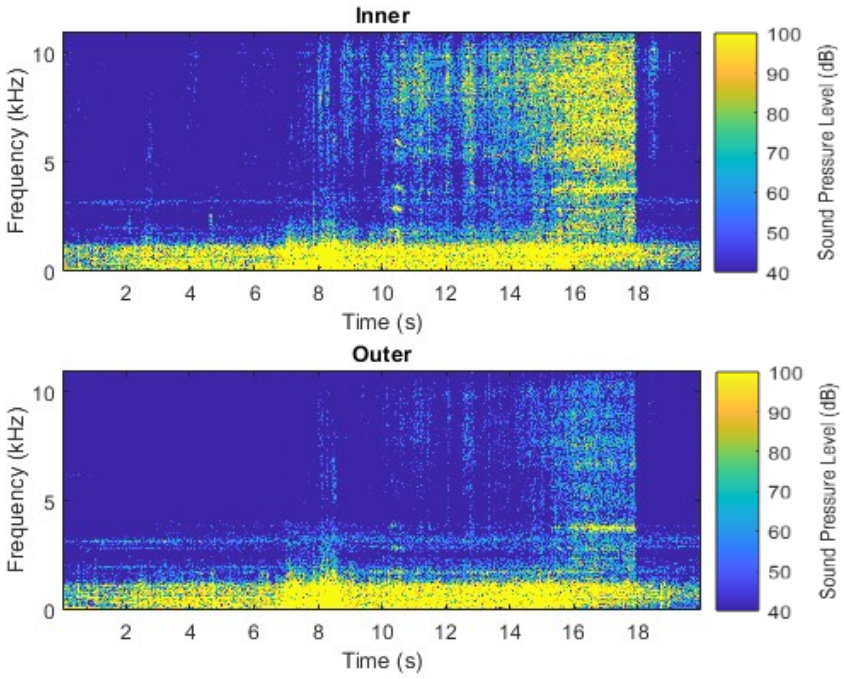

Figure 4.4: Sound pressure level spectrograms of an example curve passage that contains inner wheel squeal. QTMS passage identifier 738436439204, curve radius 178 m.

Figure 4.5 and Figure 4.6 show the spectra and spectrogram respectively for a curve passage with outer wheel squeal.

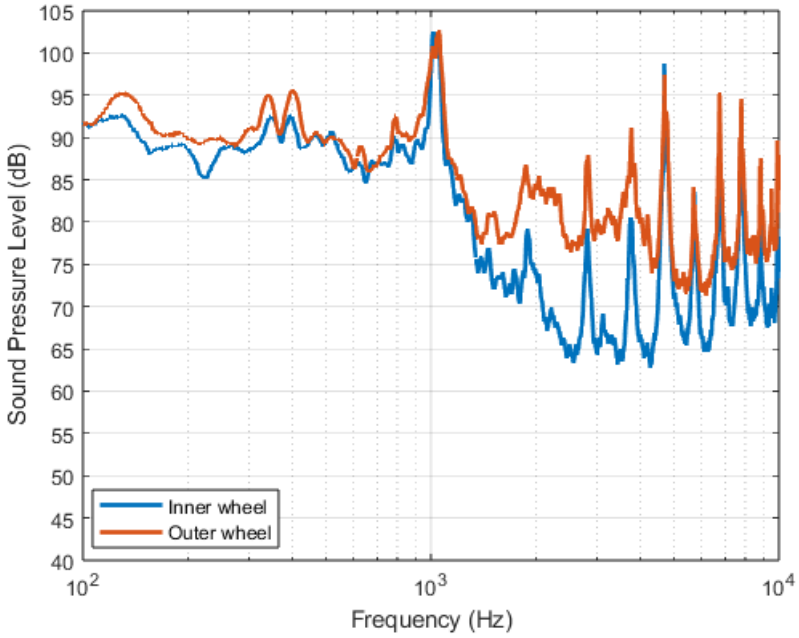

Figure 4.5: Sound pressure level spectra of an example curve passage that contains outer wheel squeal. QTMS passage identifier 738436942676, curve radius 122 m.

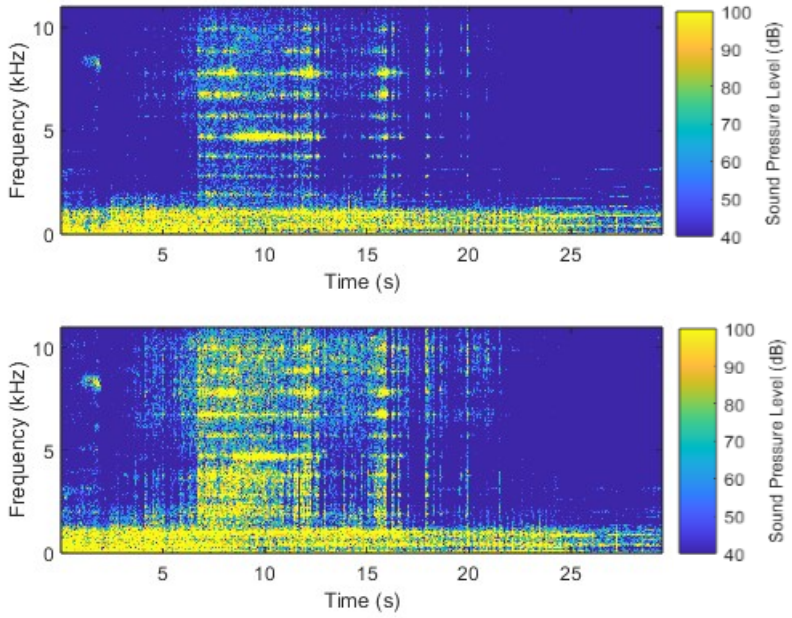

Figure 4.6: Sound pressure level spectrograms of an example curve passage that contains outer wheel squeal. QTMS passage identifier 738436942676, curve radius 122 m.

Figure 4.7 and Figure 4.8 show the spectra and spectrogram respectively for a curve passage without squeal.

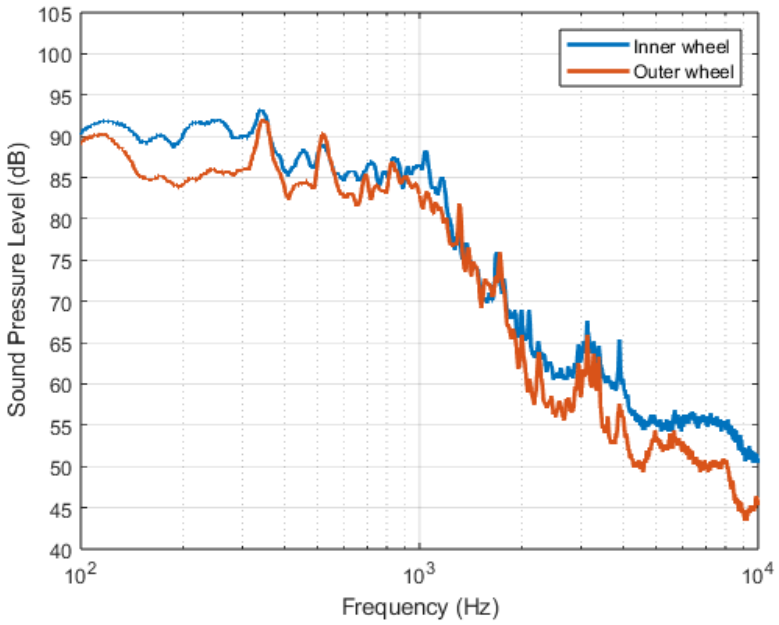

Figure 4.7: Sound pressure level spectra for an example curve passage that does not contain squeal. QTMS passage identifier 738435652240, curve radius 150 m.

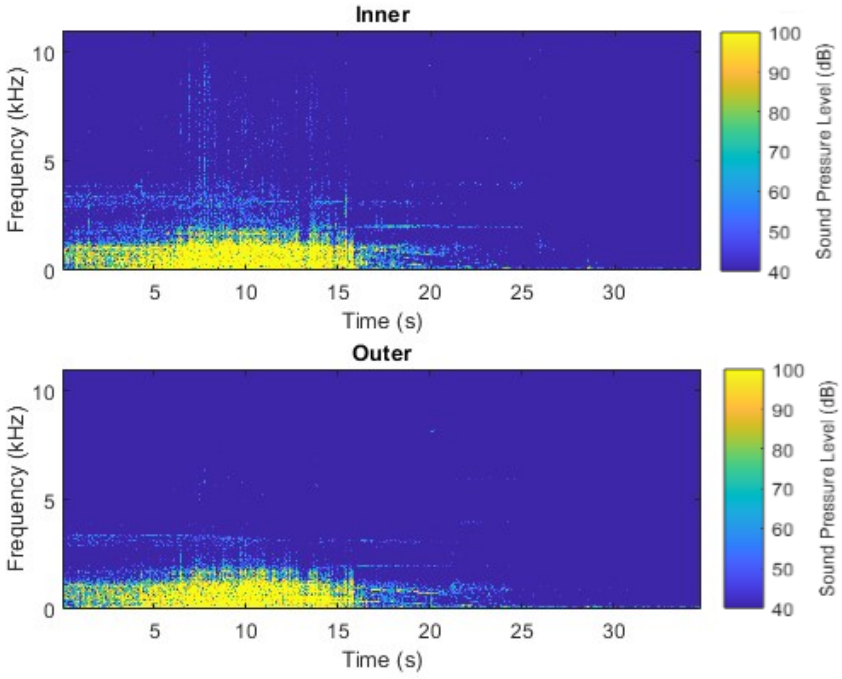

Figure 4.8: Sound pressure level spectrograms for an example curve passage that does not contain squeal. QTMS passage identifier 738435652240, curve radius 150 m.

4.2 Inner wheel squeal detection methods

Method A was used as baseline as stated earlier. Figures 4.9-4.12 show examples of vehicle passages with inner wheel squeal detected by method A in curves belonging to curve radius categories 1-4 (for a description of curve radius categories see Table 3.1. The spectrogram of the passage through the curve radius category 4 curve shown in Figure 4.12 presents almost no visible squeal.

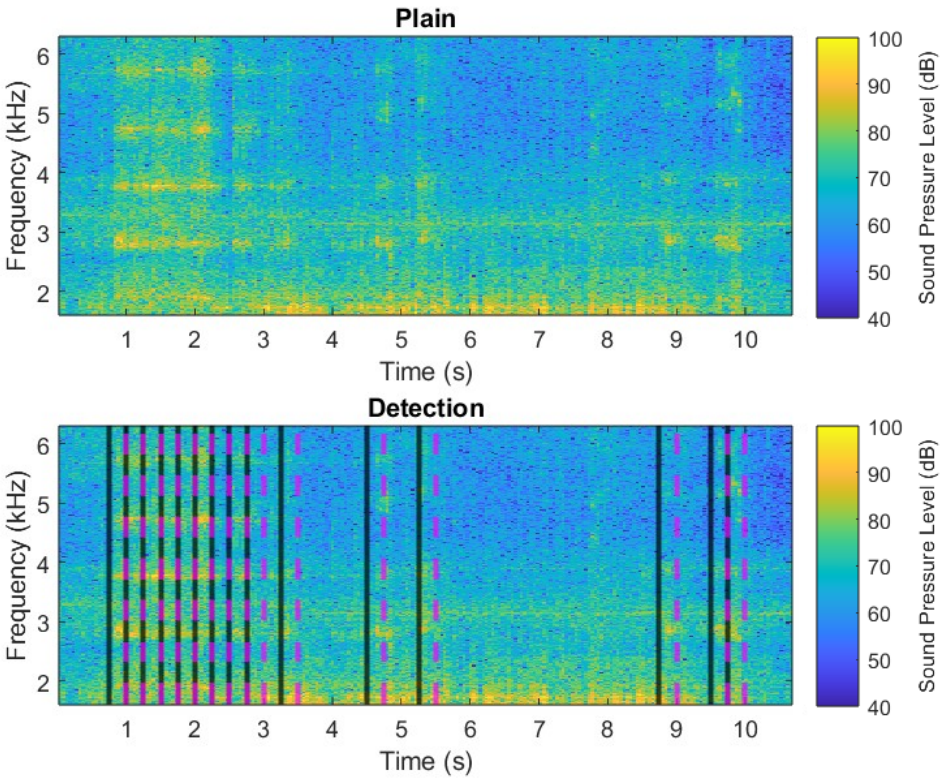

Figure 4.9: Curve radius category 1 (curve radius between 101-200 m), QTMS passage identifier 738446019067, curve radius 150 m.

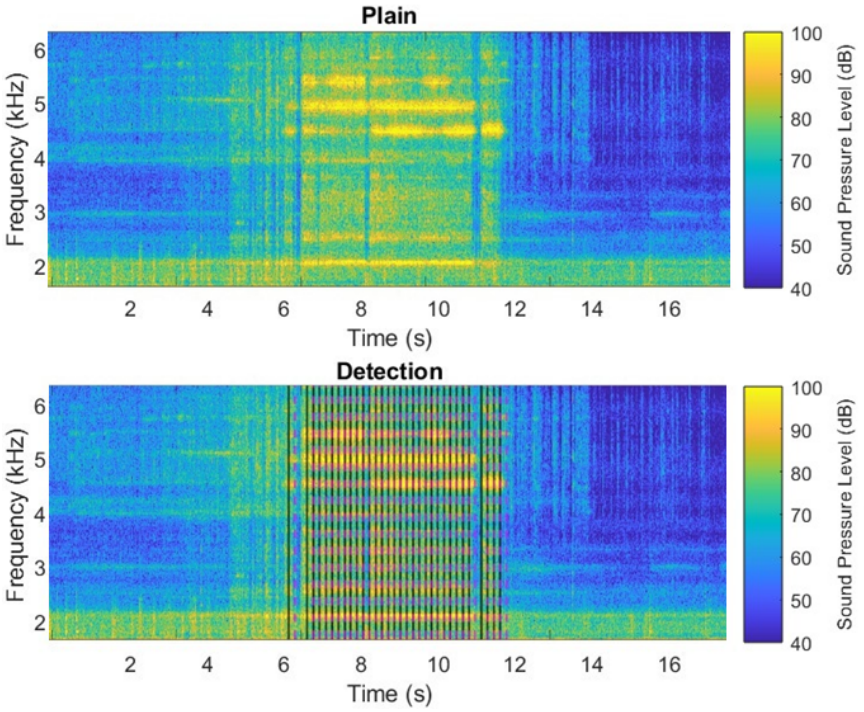

Figure 4.10: Curve radius category 2 (curve radius between 201-300 m), QTMS passage identifier 738440338536, curve radius 213 m.

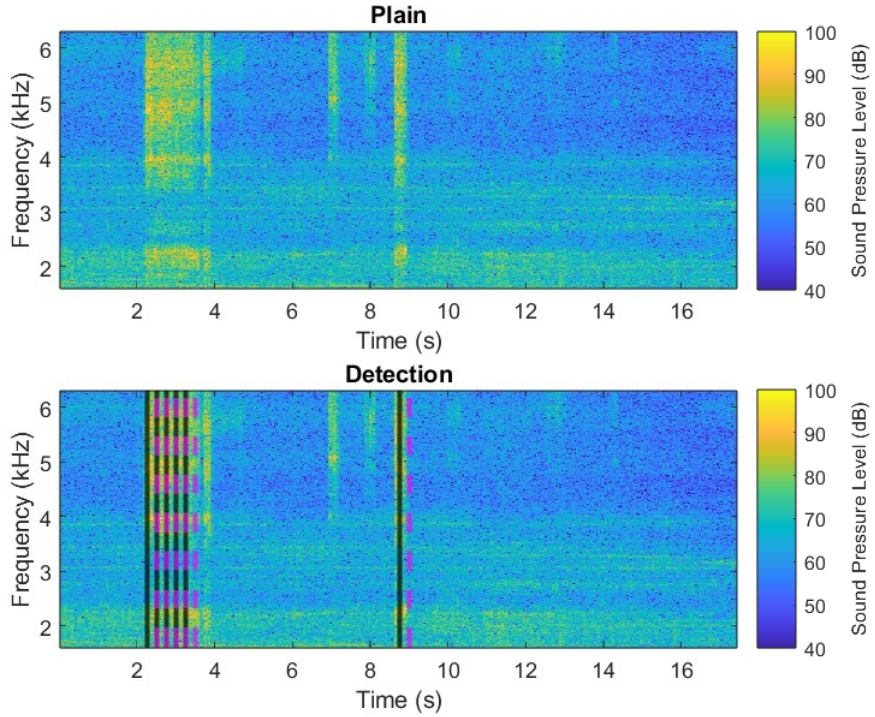

Figure 4.11: Curve radius category 3 (curve radius between 301-400 m), QTMS passage identifier 738435548074, curve radius 352 m.

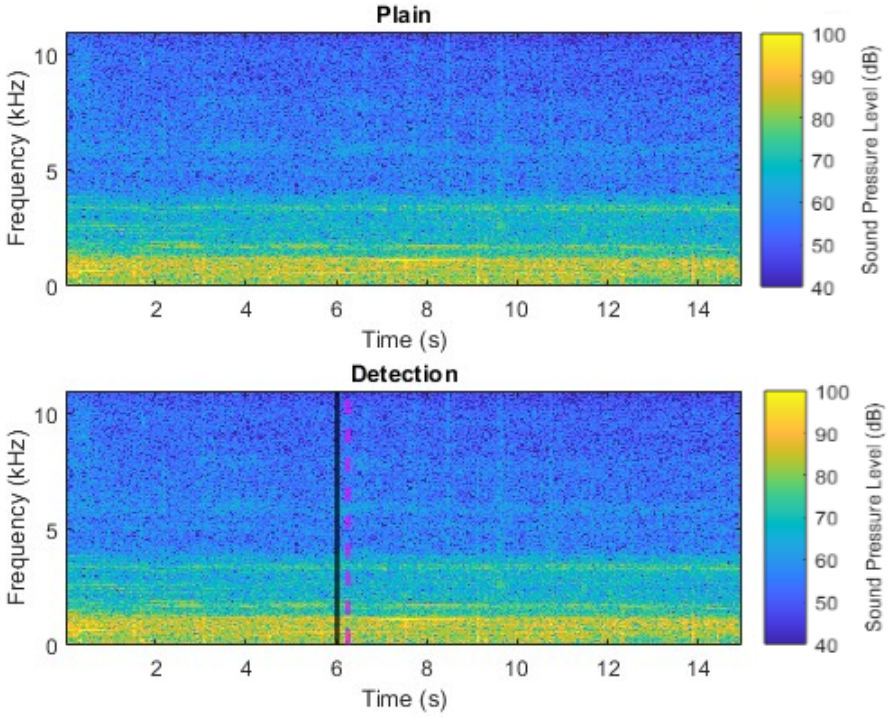

Figure 4.12: Curve radius category 4 (curve radius between 401-500 m), QTMS passage identifier 738435793265, curve radius 460 m.

Table 4.1 shows the number of passages containing at least one instance of detected inner wheel squeal, according to the different methods.

Table 4.1: Number of inner wheel squeal detections for each of the three methods.

		Method A	**Method B**	**Method C**
Name	Total	No. of detections	No. of detections	No. of detections
Cat 1	431	84% (361)	3% (11)	96% (412)
Cat 2	854	68% (577)	2% (13)	99% (850)
Cat 3	1455	21% (309)	2% (33)	98% (1429)
Cat 4	610	1% (8)	4% (23)	83% (507)

Figure 4.13 shows an example vehicle passage from curve radius category 1 when inner wheel squeal was detected only by method B, whereas Figure 4.14 shows a passage when inner wheel squeal was detected for both method A and method B. Figure 4.13 shows a peak in sound pressure level at approximately 1000 Hz which falls outside the frequency range covered by method A. The larger energy content in the high frequency range of Figure 4.14 as compared to Figure 4.13 is noticed.

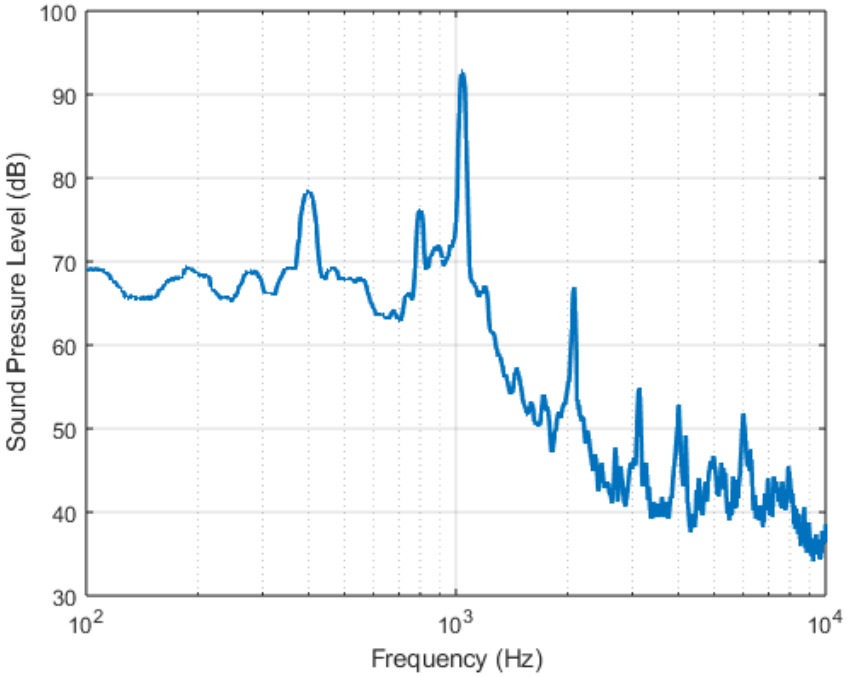

Figure 4.13: Sound pressure level spectrum for an example when method B identified inner wheel squeal. QTMS passage identifier 738437931021, curve radius 115 m.

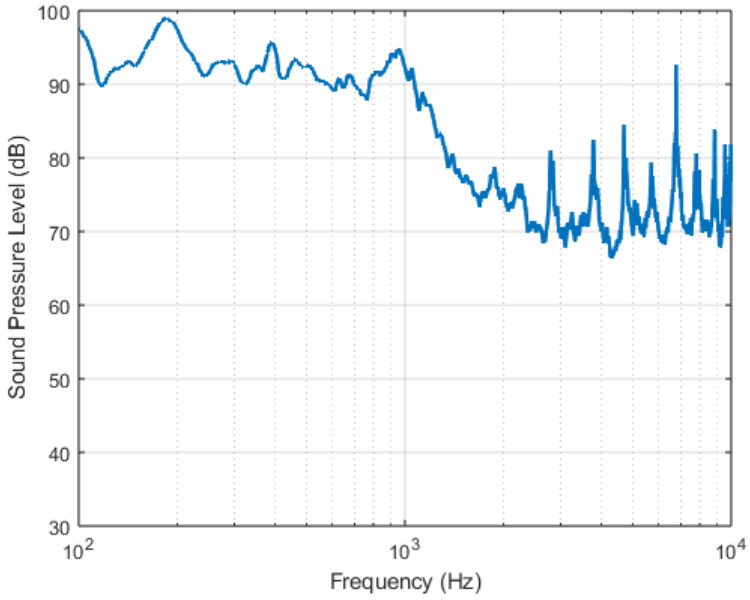

Figure 4.14: Sound pressure level spectrum for an example when method A and method B identified inner wheel squeal. QTMS passage identifier 738441551201, curve radius 118 m.

Figure 4.15 shows an example passage with inner wheel squeal identified with method B.

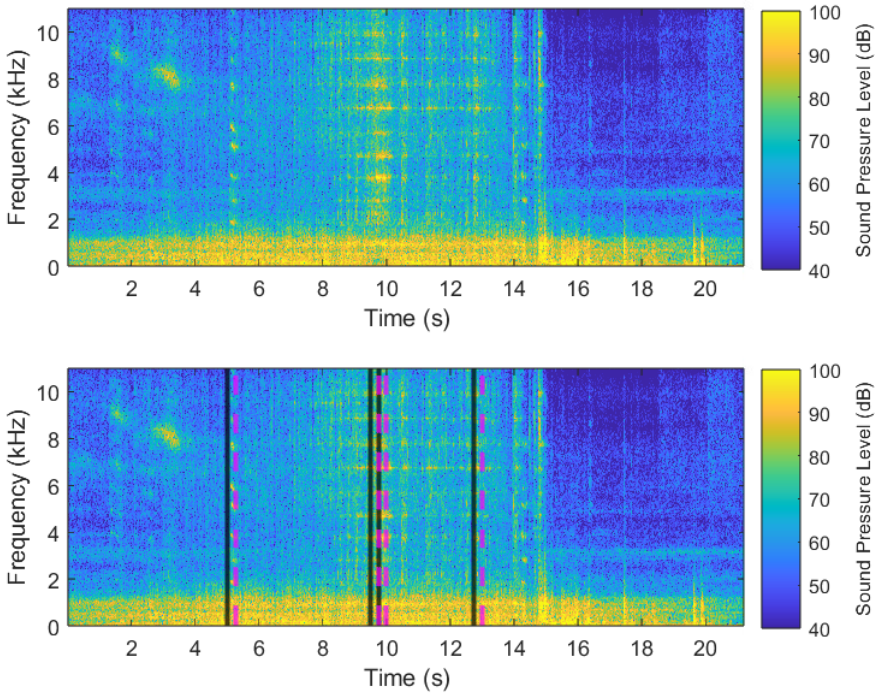

Figure 4.15: Example passage with inner wheel squeal identified with method B, QTMS passage identifier 738443656166, curve radius 118 m.

Figure 4.16-4.17 contain spectrograms with red markings for detections of inner wheel squeal identified with method C as cases when the tonality exceeds 0.4 T/-tuHMS (a further description of method C is found in Section 2.5.4) Figure 4.16-4.17 illustrate the high sensitivity of method C and explains the large number of squeal noise detections of method C observed in Table 4.1.

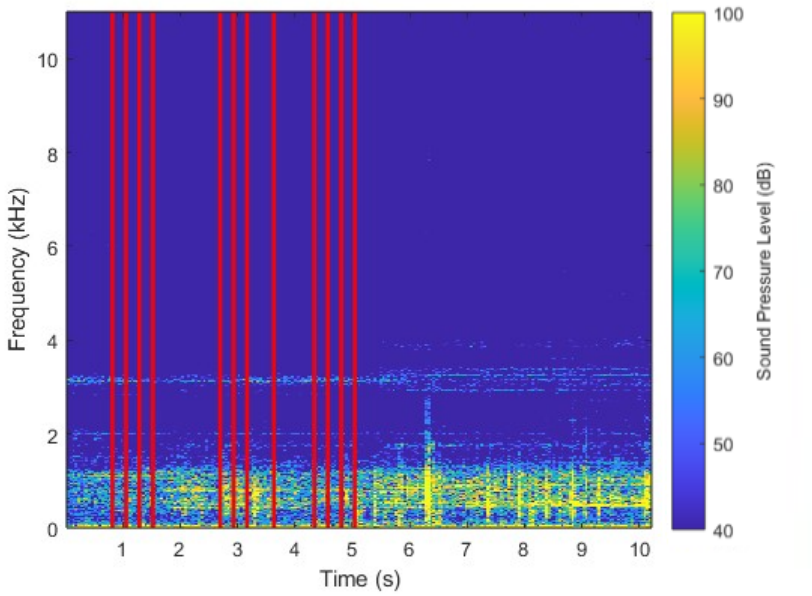

Figure 4.16: Sound pressure level spectrogram with events of inner wheel squeal identified by method C marked with red lines, QTMS passage identifier 738435530713, curve radius 300 m.

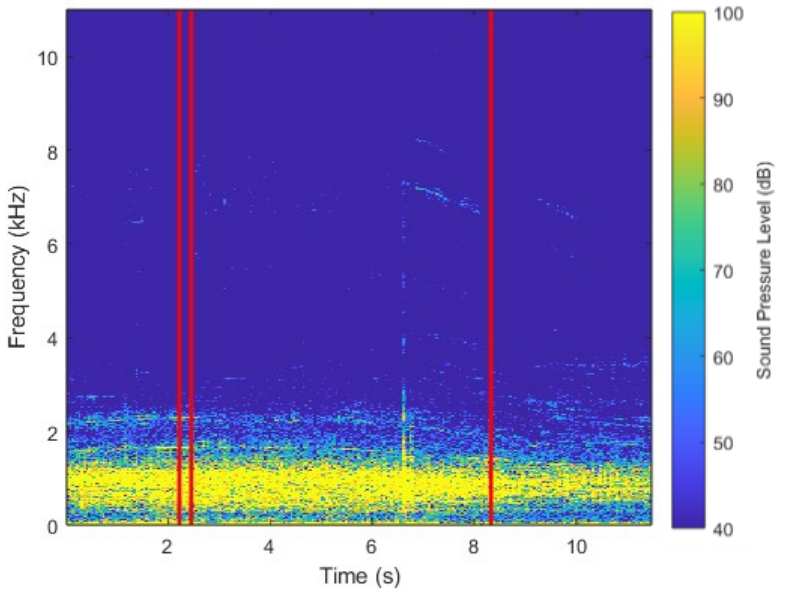

Figure 4.17: Sound pressure level spectrogram with events of inner wheel squeal identified by method C marked with red lines, QTMS passage identifier 738435666129, curve radius 433 m.

4.2.1 Assessment of method B and C

Figure 4.18 shows an example passage with inner wheel squeal identified with method C.

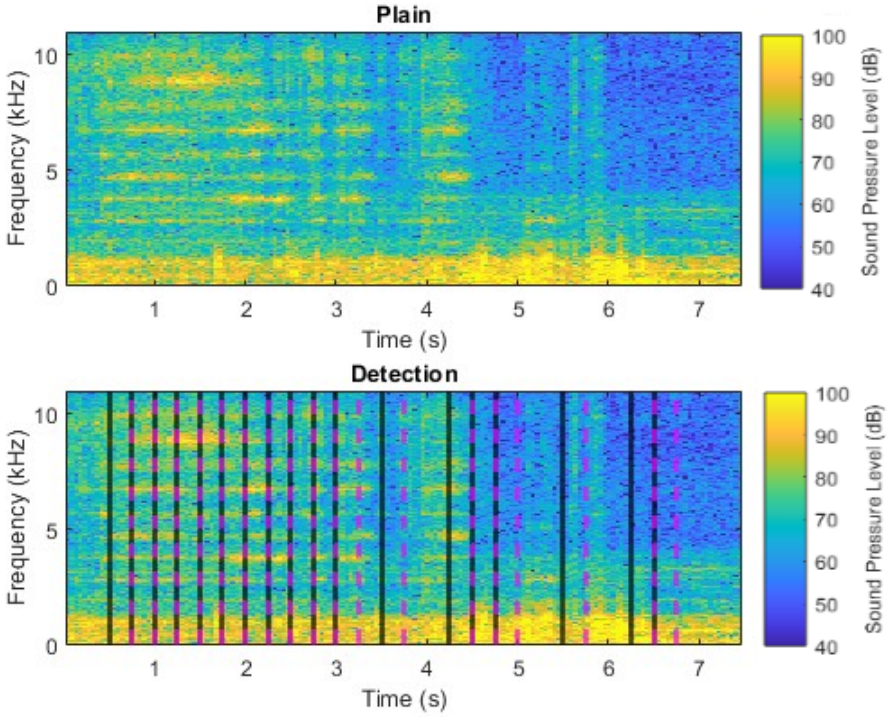

Figure 4.18: Sound pressure level spectrograms of curve passage with inner wheel squeal detected with method C. QTMS passage identifier 738435669601, curve radius 115 m.

Vehicle passages identified to contain inner wheel squeal according to method C are compared to those of method A, see Table 4.2. A description of the assessment procedure, including an explanation of True Positives (TP), True Negatives (TN), False Positives (FP) and False Negatives (FN) is found in Section 3.4.

Table 4.2: Comparison of method A and C.

Name	Total	No. of Hits	TP	FP	TN	FN
Cat 1	431	96% (412)	81% (347)	15% (65)	1% (5)	3% (14)
Cat 2	854	99% (850)	67% (575)	32% (275)	0.1% (2)	0.1% (2)
Cat 3	1455	98% (1429)	21% (305)	77% (1124)	1% (21)	0.1% (4)
Cat 4	610	83% (507)	1% (8)	82% (499)	17% (103)	0% (0)

Figure 4.19 shows an example vehicle passage with inner wheel squeal identified with method B. Table 4.3 compares the performance of method B against method A.

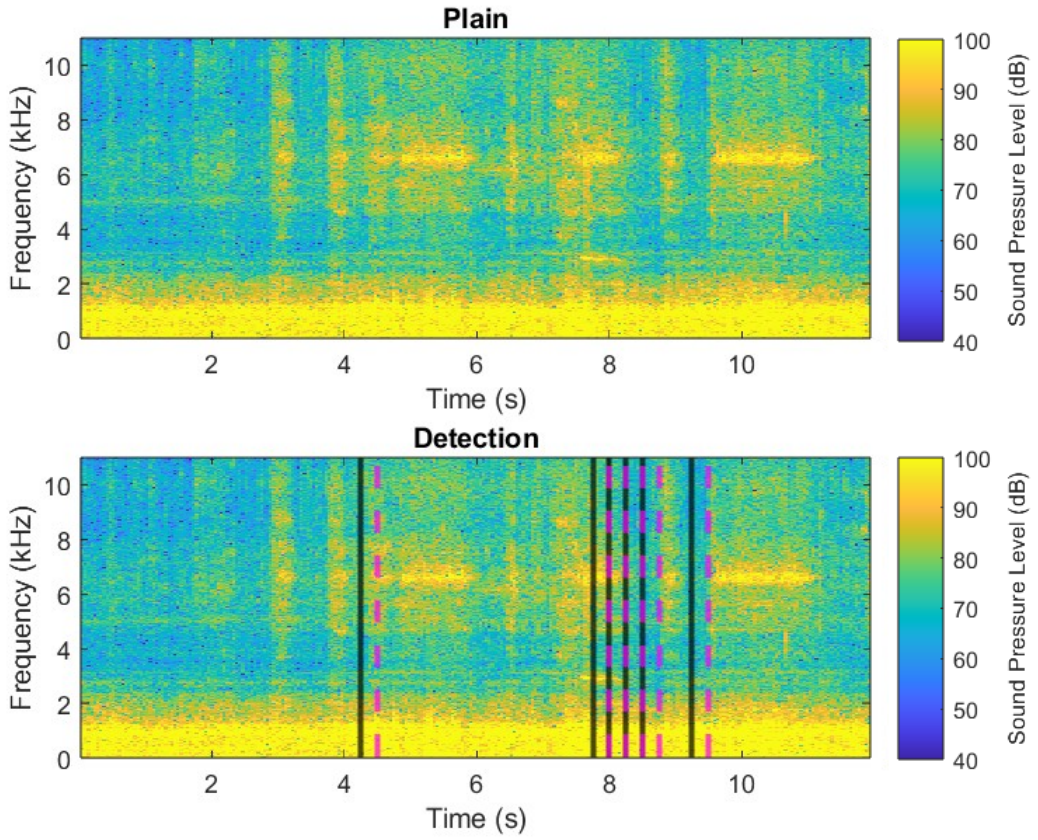

Figure 4.19: Sound pressure level spectrograms of curve passage with inner wheel squeal detected with method B. QTMS passage identifier 738435551546, curve radius 198 m.

Table 4.3: Comparison of method B against method A.

Name	Total	No. of Hits	TP	FP	TN	FN
Cat 1	431	3% (11)	2% (7)	1% (4)	15% (66)	82% (354)
Cat 2	854	2% (13)	1% (11)	0.2% (2)	32% (275)	66% (566)
Cat 3	1455	2% (33)	0.3% (5)	21% (304)	77% (1117)	2% (28)
Cat 4	610	4% (23)	0% (0)	4% (23)	95% (579)	1% (8)

Table 4.4 shows peak sound pressure levels for a few selected sections where method A has identified inner wheel squeal while method B has not. The corresponding 1/24 octave- and narrow band spectrograms are found in Appendix A.

Table 4.4: Sound pressure levels of peak and neighboring 1/24 octave-bands.

Passage	**Peak (dB)**	**Left Neighbour (dB)**	**Right Neighbour (dB)**
738456359119	95.8	82.1	90.4
738435555018	97.2	85.1	87.9
738435859237	111.5	102.2	93.4
738436359343	104.9	88.3	98.7
738437653802	94.6	84.4	86.1

Table 4.5 shows the average amount of squeal time for a passage containing inner wheel squeal according to the different methods. With regards to method B and method C only passages that fall into the True Positive category have been taken into account, while for method A all passages for which inner wheel squeal have been identified are included.

Table 4.5: Average amount of squeal time for the three methods.

Name	**Method A**	**Method B**	**Method C**
Cat 1	2.4 s	0.6 s	1.3 s
Cat 2	3.5 s	0.6 s	2.9 s
Cat 3	1.2 s	0.5 s	3.3 s
Cat 4	0.6 s	0 s	1.0 s

Table 4.6 shows the extent to which occasions of inner wheel squeal identified with methods B and C corresponds to those of method A. The comparison is based on curve squeal identification made for time instances of 0.25 s. Only cases of True Positives are accounted for.

Table 4.6: Comparison with respect to the proportion of 0.25 s time instances when inner wheel squeal has been detected by method B and method C as compared to the results of method A.

Name	**Method B**	**Method C**
Cat 1	90%	74%
Cat 2	88%	82%
Cat 3	93%	88%
Cat 4	0%	90%

4.2.2 Alternative implementations of method B

Two alternative implementations of method B has been implemented corresponding to (1) a decrease of the threshold on level difference between the peak and neighboring 1/24-bands from 10 dB to 3 dB and (2) the application of the Wollongong criterion for flange squeal to identify curve squeal noise radiated from the inner wheel (Section 2.5.2). Results for alternative 1 and 2 are presented in Figure 4.20 and Table 4.7, and Figure 4.21 and Table 4.8, respectively. It is quite clear that neither alternative yield a satisfying result. Alternative 1 tops out at 50% for category one before showing a decay in accuracy as the radii of the curves increase. Alternative 2 provides poor results throughout all categories.

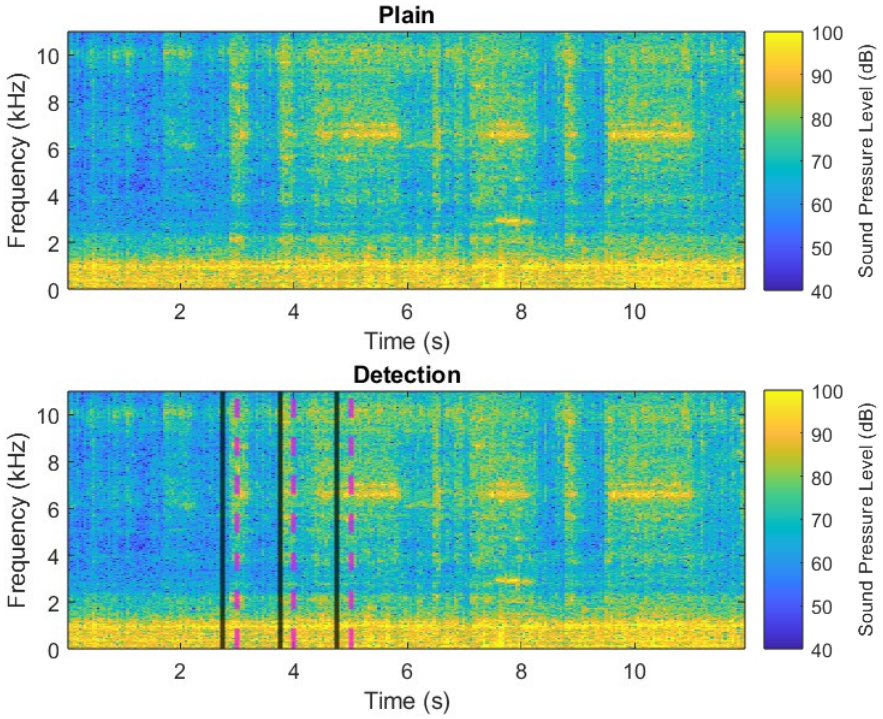

Figure 4.20: Method B modified with a decreased threshold on noise level difference to 3 dB, QTMS passage identifier 738435551546, curve radius 198 m.

Table 4.7: Comparison of Method B modified with a decreased threshold on noise level difference to 3 dB and method A.

Name	Total	No. of Hits	TP	FP	TN	FN
Cat 1	431	61% (261)	50% (215)	11% (46)	6% (24)	34% (146)
Cat 2	854	44% (376)	34% (293)	10% (83)	23% (194)	33% (284)
Cat 3	1455	39% (571)	10% (146)	29% (425)	50% (720)	11% (163)
Cat 4	610	42% (254)	0.5% (3)	41% (251)	58% (351)	0.8% (5)

Table 4.8: Average squeal time length of method B modified with a decreased threshold on noise level difference to 3 dB compared to method A.

Name	Avg. Squeal Time (s)	Avg. Similarity (%)
Cat 1	1.4	81
Cat 2	2.9	79
Cat 3	1.2	85
Cat 4	1.8	60

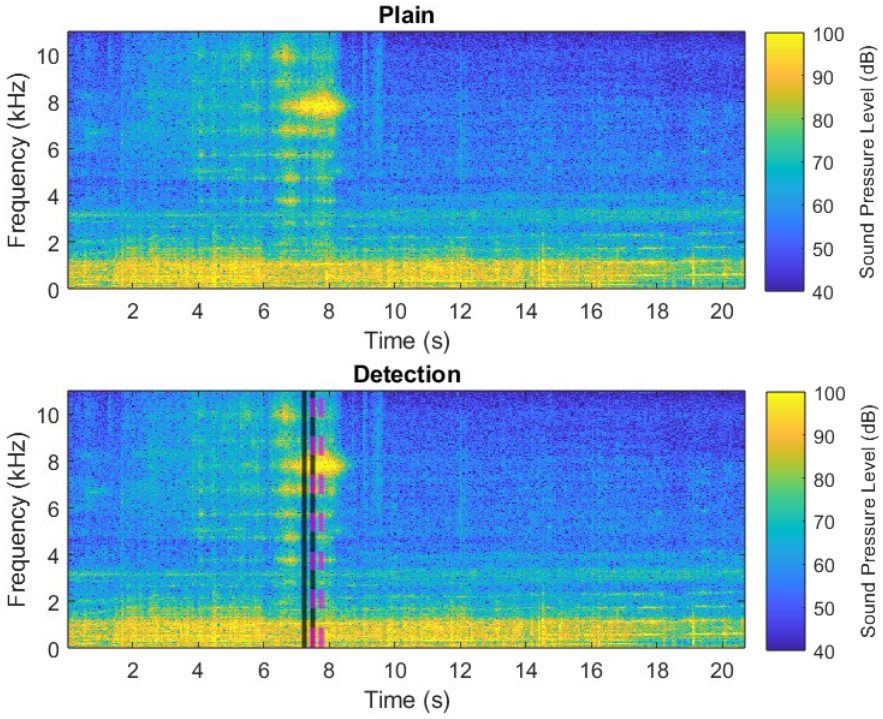

Figure 4.21: The criterion of method B for detection of flange noise applied for the identification of curve squeal from the inner wheel, QTMS passage identifier 738435551546, curve radius 198 m.

Table 4.9: Assessment of the application of the flange noise identification criterion of method B for the detection of curve squeal from the inner wheel. Comparison towards method A.

Name	Total	No. of Hits	TP	FP	TN	FN
Cat 1	431	4% (16)	4% (16)	0% (0)	16% (70)	80% (345)
Cat 2	854	11% (91)	11% (90)	0.1% (1)	32% (276)	57% (487)
Cat 3	1455	6% (269)	0.1% (17)	0.1% (9)	78% (1136)	20% (292)
Cat 4	610	0.1% (2)	0% (0)	0.1% (2)	98% (600)	0.1% (8)

Table 4.10: Assessment of the application of the flange noise identification criterion of method B for the detection of curve squeal from the inner wheel. Comparison towards method A with respect to average squeal time length.

Name	Avg. Squeal Time (s)	Avg. Similarity (%)
Cat 1	0.6	72
Cat 2	3.1	67
Cat 3	0.7	60
Cat 4	0	0

4.2.3 Method D

Method D evaluates the entire vehicle passage to find the highest sound pressure level, this values is then compare against a threshold, hence only one result is obtained per passage. An overview of the distribution of peak values can be found in Appendix B. Table 4.11 compares the results obtained for the peak value method against method A. Category one and two shows half decent results, hovering around 50% before declining sharply at category three and four.

Table 4.11: Comparison of the peak value method towards method A.

Name	Total	No. of Hits	TP	FP	TN	FN
Cat 1	431	50% (217)	48% (206)	3% (11)	14% (59)	36% (155)
Cat 2	854	82% (696)	57% (491)	24% (205)	8% (72)	10% (86)
Cat 3	1455	14% (200)	8% (114)	6% (86)	73% (1060)	13% (195)
Cat 4	610	0.1% (5)	0	0	99% (602)	1% (8)

4.3 Discussion of curve squeal detection methods

The literature study in Section 2.2 presents the rule of thumb by Rudd that states that curve squeal should not occur if the radius of the curve is larger than 100 times the bogie wheelbase. The bogie wheelbase of the metro train used on the green line is 2.3 m. Therefore, little to no curve squeal should occur in category three and four. A noticeable decrease in the amount of detected inner wheel squeal in curves of curve radius categories 3 and 4 can be noticed in Table 4.1.

Table 4.3 and 4.2 compare method B and method C against method A. Significant differences are noticed. For method B, Table 4.3 shows its low number of detections as the main reason. This may be related to the method being developed for trackside instead of onboard application in such way that. As a trackside method may need to focus more on detecting the onset and offset of external sounds, rather than just the target sound. Thus the method may overcompensate certain filter settings that while helpful when trackside may be a detriment when onboard.

For many cases where method A has detected inner wheel squeal, the gap between the peak and neighboring 1/24 octave bands is not sufficiently large to meet the criterion of method B, see Table 4.4 and Appendix A. A general observation is that the squeal noise recorded on the Stockholm metro seems to have a more broadband character then optimal with respect to method B.

As for method B, method C covers the frequency range up to 10 kHz however it shows the opposite behavior with a consistently high number of detected curve squeal events, see Table 4.2. This is particularly pronounced for curves with large radius. The prospect of combining method C with a limit in frequency range was explored but did not have a significant impact on the accuracy.

Table 4.5 shows the average squealing time length of all evaluated methods. A difference of roughly a second across all methods is noticed, with method B being most consistent across the curve radius categories. This is since most of its detections only contain one instance of squeal.

The True Positive of method B and C were compared against method A to see if they detected squeal at the same times instances during passages. Table 4.6 shows that the methods match quite well. The reason is due to the fact that for most passages neither method identifies squeal.

Two alternative implementations of method B were tested, see Table 4.7. To better capture the more broadband character of inner wheel squeal at the Stockholm metro the threshold on sound pressure level of neighboring 1/24-bands was lowered from 10 dB to 3 dB. The results showed a large increase in number of squeal detections and as well as an increase in the number of True Positives. Despite the increase in number of squeal detections still the difference with respect to method A was shown to be significant. The flange squeal detection algorithm of method B was applied to identify inner wheel squeal. Table 4.9 shows the number of curve squeal detections

using this modified version of method B being far from those obtained with method A. The reason for this stems from the large amount of energy found in the low frequency rolling noise which makes squeal with very high level components in the high frequency range being able to satisfy the flange squeal criterion of method B.

Table 4.11 shows that the peak value method compares rather well with method A. Almost all of the detected squealing passages are noticed to fall into the True Positive category. The downside of the method is that it is limited to the assessment of entire vehicle passages. Moreover, looking at the diagrams of Appendix B, the number of cases with peak noise levels exceeding 95 dB decreases with higher radii following the rule of thumb established by Rudd.

4.4 Outer wheel squeal detection methods

The assessment of methods to detect outer wheel squeal presented below is performed by visual analysis of a small sample of randomly selected curve passages of each curve radius category. The methods for detection of outer wheel squeal accounted for in the analysis are: A (Section 2.5.1), B (Section 2.5.2) and C (Section 2.5.3).

Tables 4.12-4.15 contain information on the number of curve passages detected to have at least one instance of outer wheel squeal according to the different methods. To ensure that there are no false positives present in the results, the passages where method A has detected inner wheel squeal have been filtered out. Figure 4.22-4.25 show spectrograms of example vehicle passages for which outer wheel squeal has been detected.

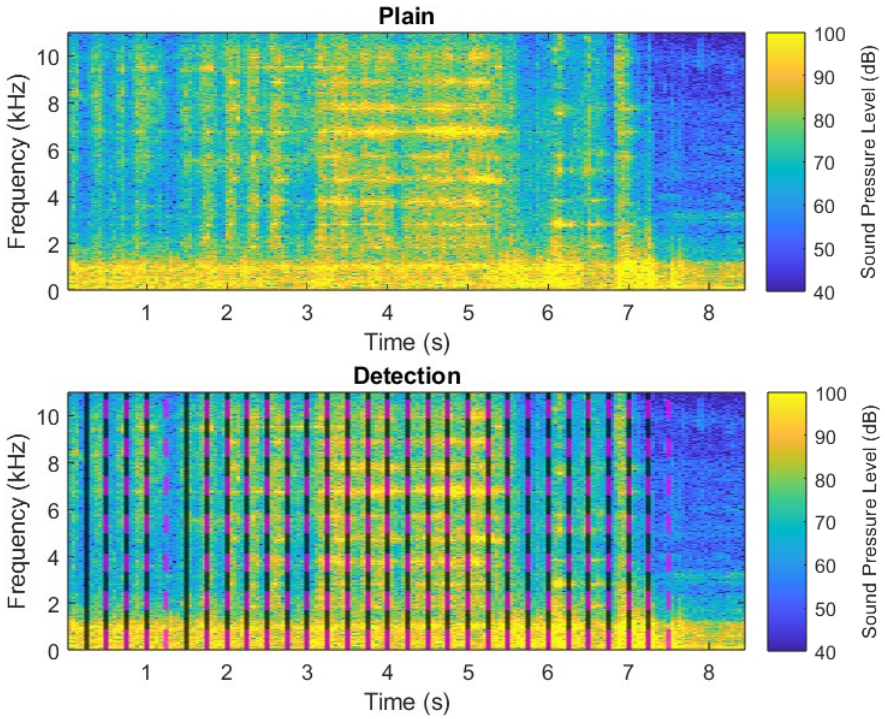

Figure 4.22: Inverse method A for detection of outer wheel squeal, QTMS passage identifier 738435762015, curve radius 115 m.

Table 4.12: Summary of results with respect to outer wheel squeal detected by application of inverse method A. Passages with inner wheel squeal have been excluded.

Category	Total no. of passages	No. of detections
Cat 1	431	15% (64)
Cat 2	854	11% (94)
Cat 3	1455	4% (60)
Cat 4	610	0.3% (2)

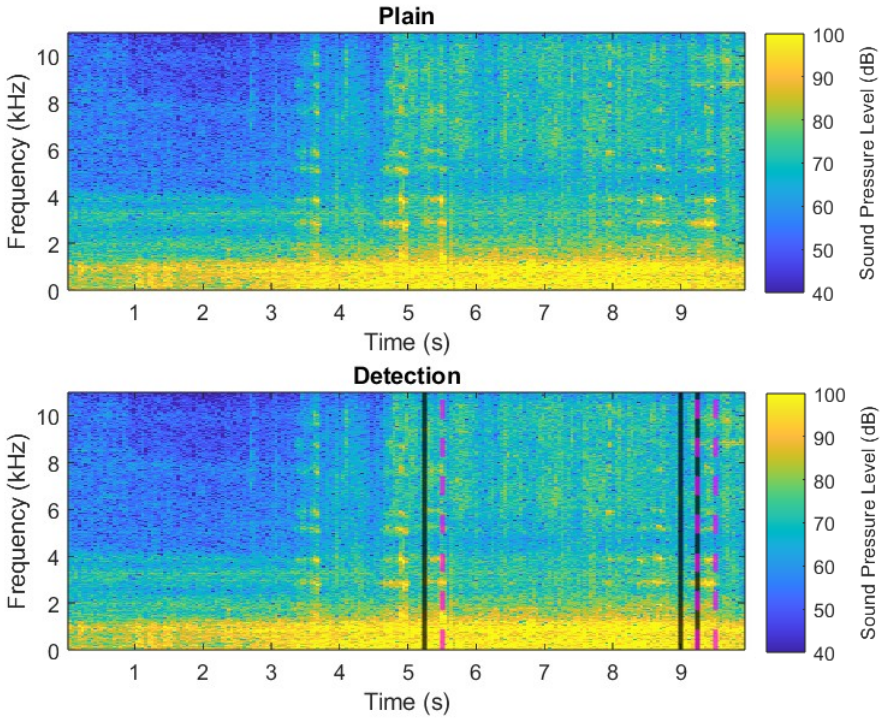

Figure 4.23: Method C for detection of outer wheel squeal, QTMS passage identifier 738435624463, curve radius 150 m.

Table 4.13: Summary of results with respect to outer wheel squeal detected by method C. Passages with inner wheel squeal have been excluded.

Category	Total no. of passages	No. of detections
Cat 1	431	15% (65)
Cat 2	854	31% (262)
Cat 3	1455	78% (1140)
Cat 4	610	98% (600)

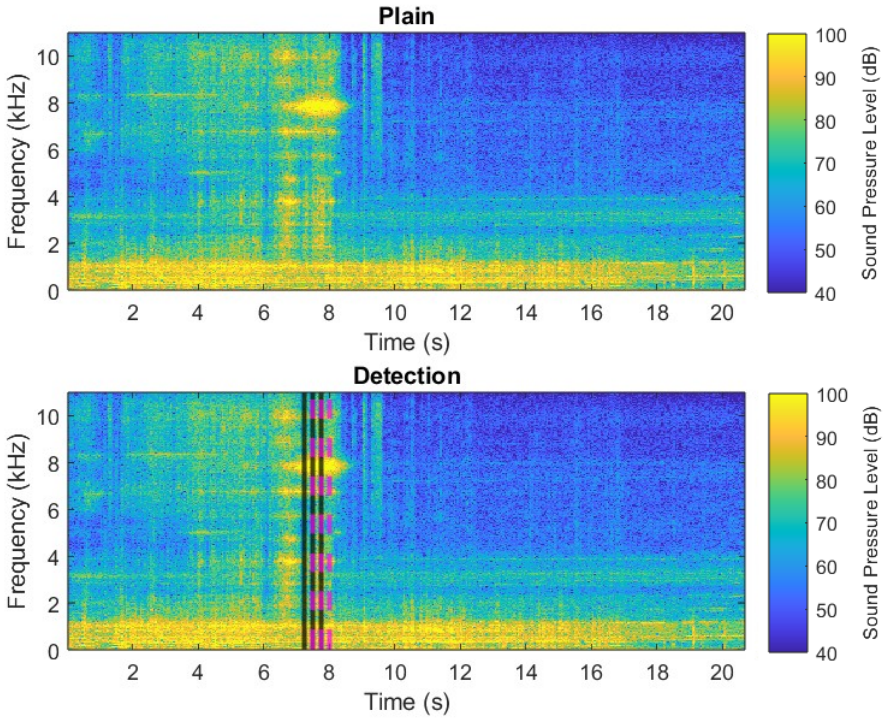

Figure 4.24: Method B (criterion for flanging noise) for detection of outer wheel squeal, QTMS passage identifier 738435762015, curve radius 122 m.

Table 4.14: Summary of results with respect to outer wheel squeal detected by method B (criterion for flanging noise). Passages with inner wheel squeal have been excluded.

Category	Total no. of passages	No. of detections
Cat 1	431	5% (23)
Cat 2	854	0% (0)
Cat 3	1455	0.7% (10)
Cat 4	610	0.3% (2)

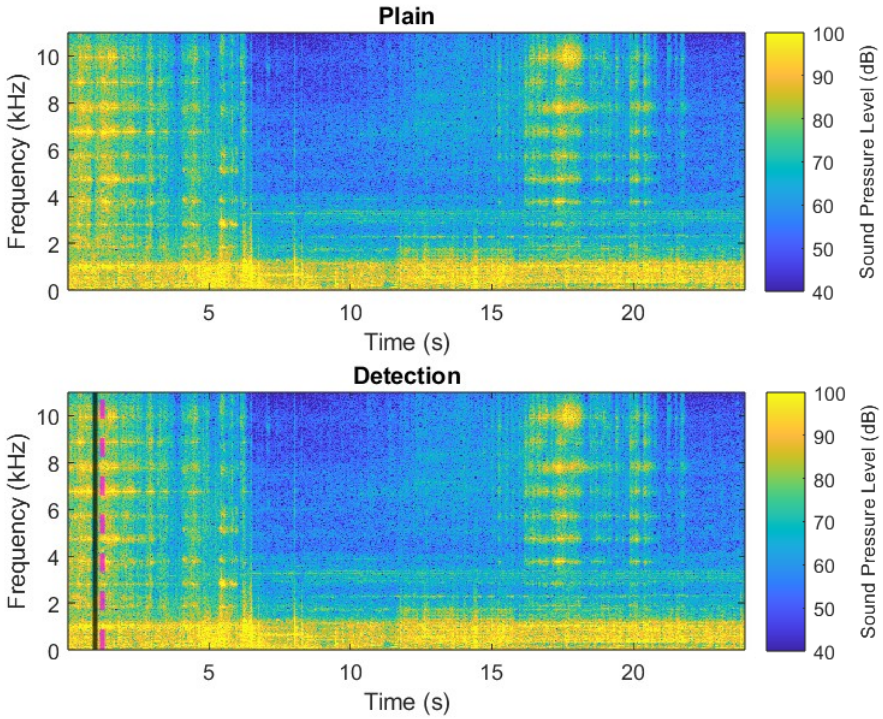

Figure 4.25: Method B (criterion for inner wheel squeal) for detection of outer wheel squeal, QTMS passage identifier 738435859237, curve radius 115 m.

Table 4.15: Summary of results with respect to outer wheel squeal detected by method B (criterion for inner wheel squeal). Passages with inner wheel squeal have been excluded.

Category	Total no. of passages	No. of detections
Cat 1	431	4% (17)
Cat 2	854	0.1% (6)
Cat 3	1455	3% (41)
Cat 4	610	2% (12)

To compare the performance of the different methods for detection of outer wheel squeal ten passages of each curve radius category were randomly selected. These passages were manually screened for outer wheel squeal by listening and inspecting spectrograms. If suspected squeal was found it would be noted down. After inspecting all ten passages in a category. The amount of passages with manually detected content of outer wheel squeal is compared to the total number of passages in order to assess the accuracy of the method in question. Results are presented in Table 4.16.

Table 4.16: Amount of clearly visible outer wheel squeal following the outlined criteria for the filtered results.

Name	Cat 1	Cat 2	Cat 3	Cat 4
Inverse Method A	80%	20%	20%	0%
Method C	70%	20%	10%	0%
Method B Flange	100%	-	50%	0%
Method B Squeal	80%	20%	10%	0%

In order to create a more robust method, Method E, for outer wheel squeal detection, the criteria of inverse method A and method B for flange squeal where combined into one. Here method A was used as basis to filter out sections of passages when this criterion was not met in order to remove the possibility of false positives. The parts that passed the first criterion were then analyzed by method B for flange squeal. Following this procedure it was not necessary to limit the analysis to curves without inner wheel squeal enabling the new algorithm to run on all passages. Table 4.17 shows the results from the new hybrid algorithm for the different curve radius categories.

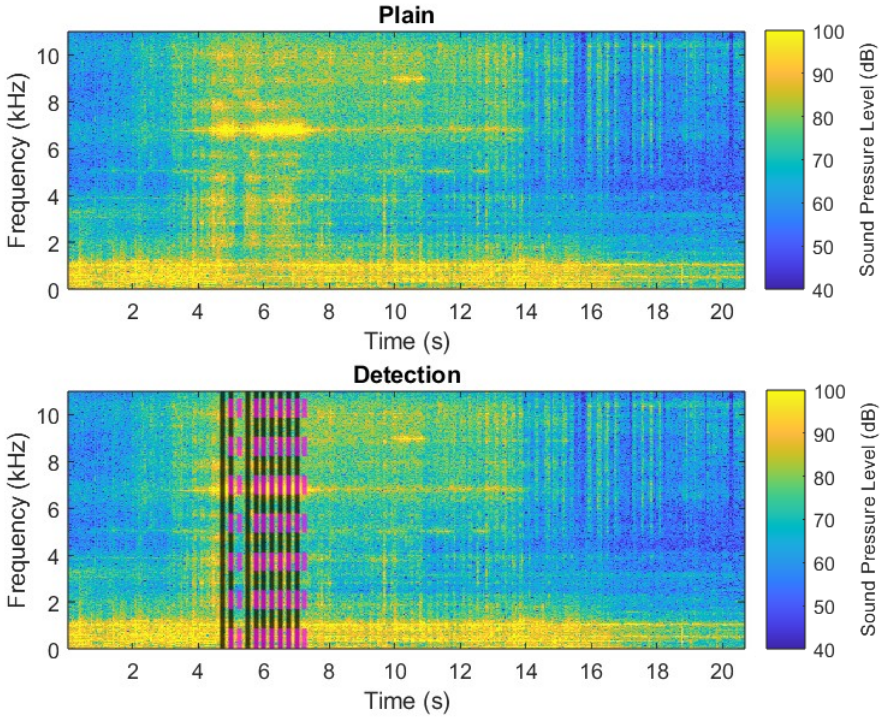

Figure 4.26: Example of outer wheel squeal detected with the hybrid method, QTMS passage identifier 738436407954, curve radius 122 m.

Table 4.17: Example of outer wheel squeal detected with the hybrid method, QTMS passage identifier 738436407954, curve radius 122 m.

		Method E
Name	Total	No. of detections
Cat 1	431	5% (23)
Cat 2	854	1% (9)
Cat 3	1455	1% (15)
Cat 4	610	0.3% (2)

Table 4.18 assesses the accuracy of the hybrid method.

Table 4.18: Amount of clearly visible outer wheel squeal following the outlined criteria.

Name	Cat 1	Cat 2	Cat 3	Cat 4
Method E	100%	100%	60%	0%

Table 4.19 presents the average length of squeal time for the different methods assessed to investigate outer wheel squeal. Vehicle passages which contain inner wheel squeal have been filtered out except for the Hybrid algorithm.

Table 4.19: Comparison of average time length of outer wheel squeal detected with the different methods.

Name	Cat 1	Cat 2	Cat 3	Cat 4
Inverse Method A	5.0 s	3.5 s	3.6 s	4.3 s
Method C	2.0 s	3.3 s	5.3 s	5.2 s
Method B Flange	1.7 s	-	1.2 s	1.5 s
Method B Curve	0.7 s	0.7 s	0.7 s	0.5 s
Method E	1.8 s	2.6 s	1.1 s	1.5 s

4.5 Discussion of outer wheel squeal detection methods

Outer wheel/flange squeal is less investigated in literature as compared to inner wheel/curve squeal. As part of the current work several observations of outer wheel squeal on the Stockholm metro are reported, see e.g. Figures 4.5 and Figure 4.6 as well as Tables 4.12-4.14.

Table 4.12-4.15 provide results on the number of vehicle passages for which outer wheel squeal has been detected. Method B using the flange squeal criterion shows the same shortcomings as were found with respect to inner wheel squeal where the large energy content in the low frequency range due to rolling noise resulted in few detections of squeal noise.

As for inner wheel squeal, method C generates a too-high number of outer wheel squeal detections. This may stem from the fact that Artemis SUITE is not originally intended to be used to detect squeal and may simply not be a suited for that purpose. Typically passages identified to include outer wheel squeal events by method C seems to include tonal components of other kind that related to squeal.

Inverse method A gives results that contain a mixture of clear cases of outer wheel squeal, no squeal cases as well as some that are difficult to manually assess, see Table 4.16. While marginally better then method C, in terms of accuracy and by a great deal regarding false positives. It still falls behind method B.

When it comes to the accuracy of the different methods, ten randomly selected samples were examined for clearly visible flange squeal, like for curve squeal. The results for the different methods and categories are presented in Table 4.16. It can be seen that the Artemis is the method with the lowest accuracy for the selected parameters, while Wollongong flange is the best for the categories where it can be applied. As mentioned earlier since there is no data to compare against, false negatives are not accounted for and it would be of interest to test these methods in a controlled environment, which would yield a better approximation of the accuracies.

Table 4.15 shows results for the inner wheel squeal detection criterion of method B instead applied for the identification of squeal noise radiation from the outer wheel. The results are similar to those obtained for the flange squeal detection criterion of method B. However, Table 4.16 indicates that its accuracy is deficient. Thus, the criterion for flange detection of method B is superior for the detection of outer wheel squeal as compared to the criterion for curve squeal.

Based on the results in Tables 4.12-4.16, method B with the criterion for flange squeal detection performs best with respect to outer wheel squeal. However, its tendency to yield false positives unless filtered is an inherent weakness. The potential mitigation of this problem by using it in combination with the inverse of method A was investigated. In the following this procedure is referred to as the hybrid method. It was implemented by first evaluating the sound pressure level difference between the wheels only keeping sections of vehicle passages where the outer wheel exceeds the inner wheel by at least 1 dB. The flange squeal criterion of method B was than applied as a second step of the analysis. The hybrid method has been applied in an analysis of all curve passages. A high accuracy is noticed in the results presented in Table 4.17. The importance of the threshold on sound pressure level difference between the wheels has been investigated and similar results obtained for threshold values between in the range between 1-3 dB.

Table 4.19 presents the average flange squeal time calculated for the different methods. The inverse method A and method C are seen to generate longer average outer wheel squeal time length as compared to method B and the hybrid method. However as stated earlier these methods are not particularly accurate and hence the average outer wheel squeal time length is probably less accurate than that provided by method B or hybrid method.

5
Conclusion

In this work, different methods for detection of inner and outer wheel squeal have been investigated for the purpose of developing a criterion for squeal noise detection applicable to onboard noise monitoring. An implementation of the method for on-board inner wheel squeal detection in operation on the Stockholm metro, Sweden, has been used as reference (method A). In addition a method available in literature developed by a research group at the Wollongong University, Australia, (method B) and as well a method based on the commercial software Artemis SUITE (method C) have been evaluated. A simpler method (D) was also devised and evaluated. Method A focuses on the difference in sound pressure level between the inner and outer wheels while method B is based on the sound pressure level difference between 1/24-octave bands. Method C uses the functionality for identification of tonal characteristics of signals available in the software Artemis SUITE. Method D compares the overall highest sound pressure level against a threshold. In addition, the squeal noise detection performance of various modifications and combinations of methods A-C were evaluated. The technology consultancy firm Tyréns supplied the study with data recorded by the on-board noise monitoring system QTMS in operation at the Stockholm metro. Noise recordings from one vehicle in regular traffic operation on the green metro line during October in 2021 were used.

Method A was found to perform best with respect to the detection of inner wheel squeal. Moreover it provides results in terms of inner wheel squeal propensity that follow the expected inverse relationship with respect to curve radii. This desired qualitative behavior was not met by method C.

In an effort to create a more uniform baseline against which to compare, method A was chosen to serve as baseline. This due to the high level of accuracy the method provides.

Method B provided poor results with regards to inner wheel squeal in terms of accuracy. The same goes for method D, that while performing better then B still falls short.

For detection of outer wheel squeal, the so-called hybrid method proposed herein that combines functionality of method A and method B performed best. Both method A for inner wheel squeal and the hybrid method for outer wheel squeal showed best results for curve radii in the range between 101-300 m. For curves with larger radii the number of false identifications of squeal events increased (False Positives).

5.1 Future Work

In the current work, methods for detection of squeal have been evaluated for time instances of length 250 ms. This means that a squeal event of 250 ms length is sufficient for a curve passage to be identified as squealing. A suggestion for future work would be to investigate how to design a criteria that requires sustained squeal for a longer time period. Moreover, it is suggested to work further on how to utilize the tonal noise characteristics in the criteria design. The current work has only studied noise recorded from the Stockholm metro. The application of the different methods for squeal noise detection on noise obtained from other rail networks constitutes an important task for future work.

Bibliography

[1] Jakob Oertli. *Combating Curve Squeal Phase II Final Report*. Tech. rep. 2005. URL: https://uic.org/IMG/pdf/uic_soa_combatting_curve_squeal_p2.pdf.

[2] D. J. Thompson. "Railway Noise and Vibration_ Mechanisms, Modelling and Means of Control". In: (2009), pp. 315–342.

[3] The Railway Technical Website. *Bogies*. URL: http://www.railway-technical.com/trains/rolling-stock-index-l/bogies.html.

[4] M. J. Rudd. "Wheel/rail noise—Part II: Wheel squeal". In: *Journal of Sound and Vibration* 46.3 (June 1976), pp. 381–394. ISSN: 0022-460X. DOI: 10.1016/0022-460X(76)90862-2.

[5] David Hanson et al. *Curve Squeal: Causes, Treatments and Results*. Tech. rep. 2014. URL: https://www.acoustics.asn.au/conference_proceedings/INTERNOISE2014/papers/p1010.pdf.

[6] Ch Glocker, E. Cataldi-Spinola, and R. I. Leine. "Curve squealing of trains: Measurement, modelling and simulation". In: *Journal of Sound and Vibration* 324.1-2 (July 2009), pp. 365–386. ISSN: 0022-460X. DOI: 10.1016/J.JSV.2009.01.048.

[7] J A S A Volume, Harvey Fletcher, and W A Munson. *Loudness, Its Definition, Measurement and Calculation*. Tech. rep. 1933. URL: http://asadl.org/terms.

[8] International Organization for Standardization. *SS-ISO 226:2004*. 2004. URL: https://www.iso.org/standard/34222.html.

[9] Corradi et al. *Proceedings of the 8th International Conference on Structural Dynamics, EURODYN 2011 : Leuven, Belgium, 4-6 July 2011*. 2011. ISBN: 9789076019314.

[10] Inaki Merideno et al. "Constrained layer damper modelling and performance evaluation for eliminating squeal noise in trams". In: *Shock and Vibration* 2014 (2014). ISSN: 10709622. DOI: 10.1155/2014/473720.

[11] N. Vincent et al. "Curve squeal of urban rolling stock—Part 1: State of the art and field measurements". In: *Journal of Sound and Vibration* 293.3-5 (June 2006), pp. 691–700. ISSN: 0022-460X. DOI: 10.1016/J.JSV.2005.12.008.

[12] C. J.M. van Ruiten. "Mechanism of squeal noise generated by trams". In: *Journal of Sound and Vibration* 120.2 (Jan. 1988), pp. 245–253. ISSN: 0022-460X. DOI: 10.1016/0022-460X(88)90432-4.

[13] D J Thompson et al. "A State-of-the-Art Review of Curve Squeal Noise: Phenomena, Mechanisms, Modelling and Mitigation". In: 139 (2018). DOI: 10.1007/987-3-319-73411-8{_}1. URL: https://eprints.soton.ac.

uk/421407/1/P246_Thompson_A_state_of_the_art_review_of_curve_squeal_noise_FINAL.pdf.

[14] J Jiang, R Dwight, and D Anderson. *Field Verification of Curving Noise Mechanisms*. 2010, pp. 349–356. URL: https://link.springer.com/book/10.1007/978-4-431-53927-8.

[15] Dave Anderson. *Wheel squeal measurement, management and mitigation on the New South Wales rail network*. Tech. rep. 2004. URL: https://www.acoustics.asn.au/conference_proceedings/AAS2004/ACOUSTIC/PDF/AUTHOR/AC040080.PDF.

[16] D. J. Fourie et al. *Analysis of Railway Wheel-Squeal Due to Unsteady Longitudinal Creepage Using the Complex Eigenvalue Method*. 2016, pp. 57–68. URL: http://www.springer.com/series/4629.

[17] Jae Chul Kim, Yang Soo Yun, and Hee Min Noh. "Analysis of Wheel Squeal and Flanging on Curved Railway Tracks". In: *International Journal of Precision Engineering and Manufacturing* 20.12 (Dec. 2019), pp. 2077–2087. ISSN: 20054602. DOI: 10.1007/s12541-019-00225-7.

[18] Rickard Nilsson et al. *A Noise Related Track Maintenance Tool for Severe Wear Detection of Wheel-Rail Contact*. Tech. rep. 2016. URL: https://www.researchgate.net/publication/307639137.

[19] Yun Ke Luo, Lu Zhou, and Yi Qing Ni. "Towards the understanding of wheel-rail flange squeal: In-situ experiment and genuine 3D profile-enhanced transient modelling". In: *Mechanical Systems and Signal Processing* 180 (Nov. 2022), p. 109455. ISSN: 0888-3270. DOI: 10.1016/J.YMSSP.2022.109455.

[20] Eomys. *What is tonality?* URL: https://e-nvh.eomys.com/what-is-tonality/.

[21] ECMA. *Psychoacoustic metrics for ITT equipment-Part 1 (prominent discrete tones)*. Tech. rep. 2009. URL: https://www.ecma-international.org/publications-and-standards/standards/ecma-418/.

[22] ECMA. *ECMA-74 Measurement of Airborne Noise emitted by Information Technology and Telecommunications Equipment*. Tech. rep. 2009. URL: https://www.ecma-international.org/publications-and-standards/standards/ecma-74/.

[23] German institute for Standardization. *DIN 45681 Acoustics - Determination of tonal components of noise and determination of a tone adjustment for the assessment of noise immissions*. 2005. DOI: https://dx.doi.org/10.31030/9601912. URL: https://www.sis.se/produkter/metrologi-och-matning-fysikaliska-fenomen/akustik-och-bullermatning/allmant/din45681/.

[24] International Organization for Standardization. *20065:2022 Acoustics-Objective method for assessing the audibility of tones in noise-Engineering method*. Tech. rep. 2023. URL: www.iso.org.

[25] Roland Sottek and Julian Becker. *Tonal Annoyance vs. Tonal Loudness and Tonality*. 2019. URL: https://www.ingentaconnect.com/content/ince/incecp/2019/00000259/00000003/art00102.

[26] Siemens. *Critical Bands in Human Hearing*. 2019. URL: https://community.sw.siemens.com/s/article/critical-bands-in-human-hearing.

[27] International Organization for Standardization. *ISO 20065:2022*. 2022. URL: https://www.sis.se/produkter/miljo-och-halsoskydd-sakerhet/buller-med-avseende-pa-manniskor/isots-200652022/.

[28] Center for Disease Control and Prevention. *How Can we Measure Impulse Noise Properly?* July 2018.

[29] Nordtest NT Acou 112. *Acoustics: Prominence of impulsive sounds and for adjustment of LAeq*. Tech. rep. 2002. URL: www.nordtest.org.

[30] Ville Rajala and Valtteri Hongisto. "Annoyance penalty of impulsive noise – The effect of impulse onset". In: *Building and Environment* 168 (Jan. 2020), p. 106539. ISSN: 0360-1323. DOI: 10.1016/J.BUILDENV.2019.106539.

[31] Jenni Radun et al. "Acute stress effects of impulsive noise during mental work". In: *Journal of Environmental Psychology* 81 (June 2022), p. 101819. ISSN: 0272-4944. DOI: 10.1016/J.JENVP.2022.101819.

[32] Robert Bullen and Jiandong Jiang. *Algorithms for detection of rail wheel squeal Algorithms for detection of rail wheel squeal Recommended Citation Recommended Citation*. Tech. rep. 2010. URL: https://ro.uow.edu.au/eispapershttps://ro.uow.edu.au/eispapers/45.

[33] John Canny. "A Computational Approach to Edge Detection". In: *IEEE Transactions on Pattern Analysis and Machine Intelligence* PAMI-8.6 (1986), pp. 679–698. ISSN: 01628828. DOI: 10.1109/TPAMI.1986.4767851.

[34] ECMA. *Psychoacoustic metrics for ITT equipment-Part 2 (models based on human perception)*. Tech. rep. 2009. URL: https://www.ecma-international.org/publications-and-standards/standards/ecma-418/.

[35] Mikael Palo. *Condition monitoring of railway vehicles a study on wheel condition for heavy haul rolling stock*. Luleå University of Technology, 2012. ISBN: 9789174394122.

[36] W.Schwanen and A.H.W.M.Kuijpers. "Early Rail Defect Detection using Sound Measurements". In: (2016). URL: https://www.ctresources.info/ccp/paper.html?id=9061.

[37] M. Oregui et al. "Monitoring bolt tightness of rail joints using axle box acceleration measurements". In: *Structural Control and Health Monitoring* 24.2 (Feb. 2017). ISSN: 15452263. DOI: 10.1002/stc.1848.

[38] Tyréns. *Quiet Track Monitoring System*. URL: https://qtms.tyrens.com/en/about-qtms/.

[39] Cordis. *Quiet Tracks for Sustainable Railway Infrastructures*. 2016. URL: https://cordis.europa.eu/project/id/604891.

[40] Kungliga Tekniska högskolan. *Banor och Linjer*. URL: https://people.kth.se/~e95_lra/tunnelbana/text/bl.html.

[41] Erik Magni Vinberg, Michael Martin, and Alfi Hadi Firdaus. *Railway Applications of Condition Monitoring*. Tech. rep. 2018. DOI: 10.13140/RG.2.2.35912.62729. URL: https://www.researchgate.net/publication/322699553.

A

Appendix A

Below a case when method A detects a sequel event whereas method B does not is presented. Figures A.1-A.3 show the spectrogram of the passage, 1/24 octave band and narrowband spectra, respectively. Results are shown for a frequency range that corresponds to that of method A.

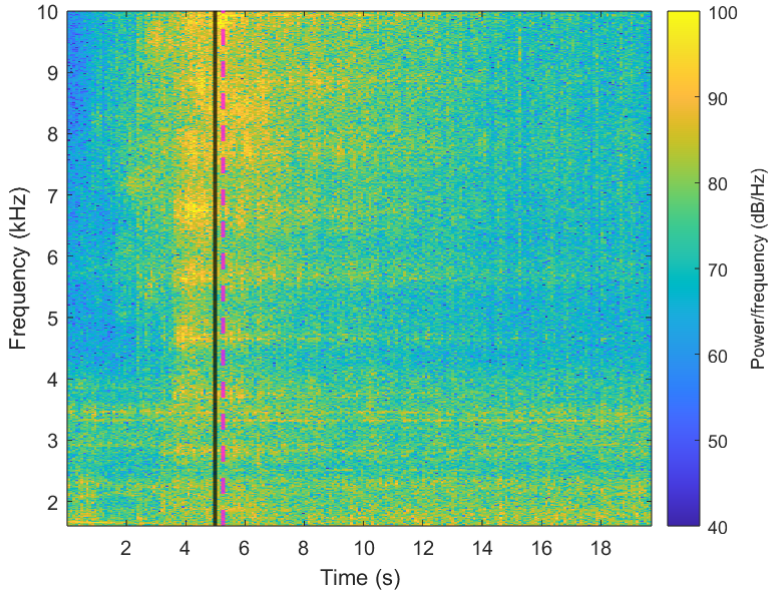

Figure A.1: Spectrogram showing a passage when method B and method A disagree on the presence of a squeal event. QTMS passage identity 738456359119, curve radius 200 m.

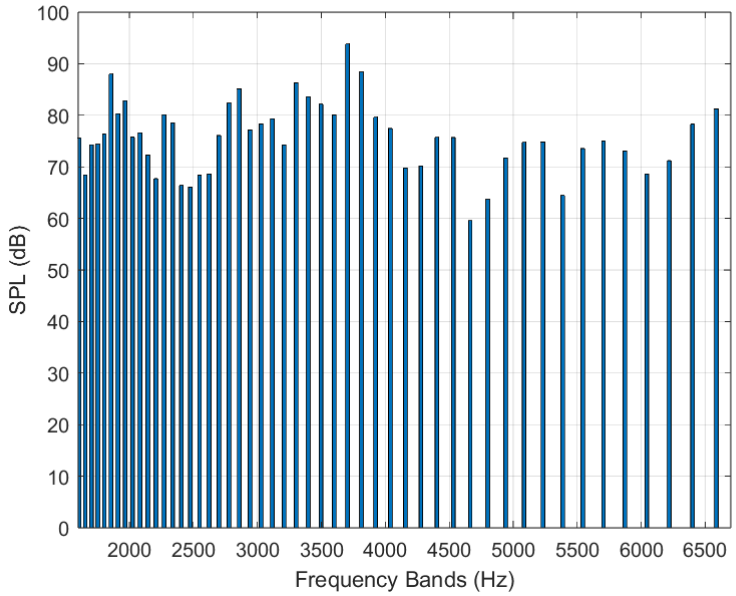

Figure A.2: 1/24 octave-band sound pressure level spectrum for the marked section in Figure A.1. QTMS passage identity 738456359119, curve radius 200 m.

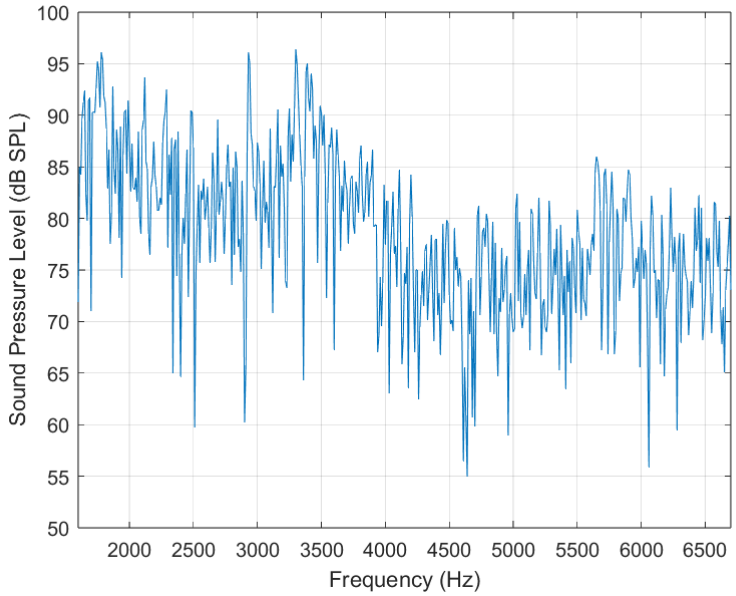

Figure A.3: Narrow-band sound pressure level spectrum of the marked section in Figure A.1. QTMS passage identity 738456359119, curve radius 200 m.

B

Appendix B

Figures B.1-B.4 show the distribution of the peak values found by the peak value method for passages in the different curve radius categories.

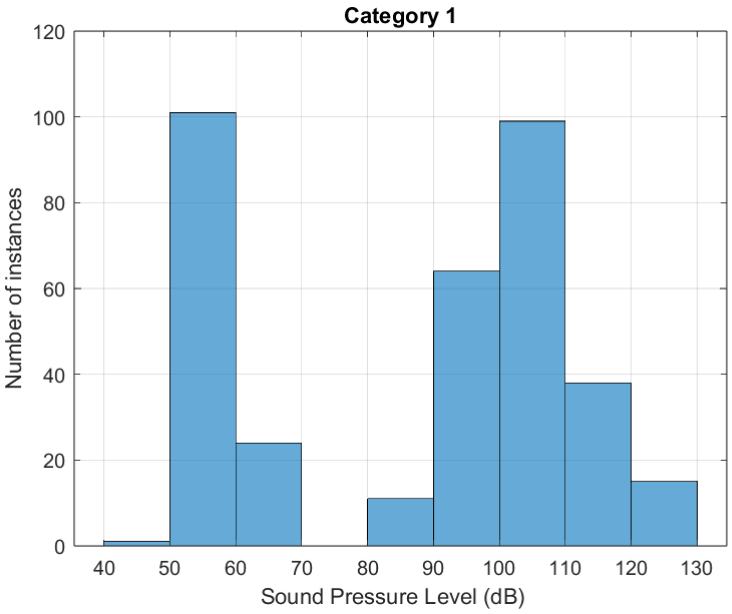

Figure B.1: Distribution of peak sound pressure levels for curve radius category 1.

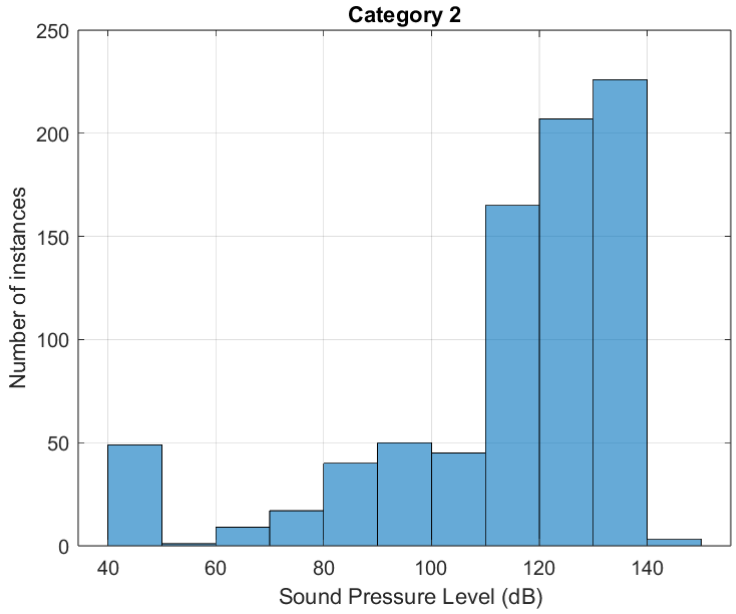

Figure B.2: Distribution of peak sound pressure levels for curve radius category 2.

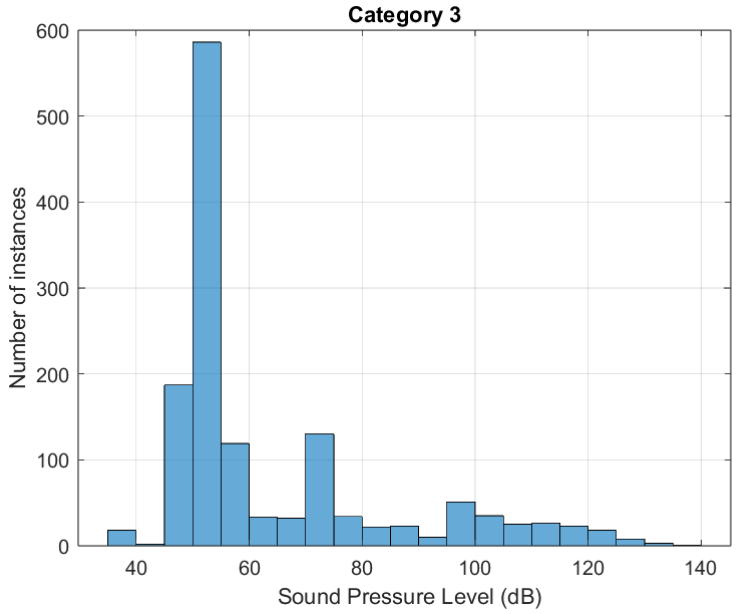

Figure B.3: Distribution of peak sound pressure levels for curve radius category 3.

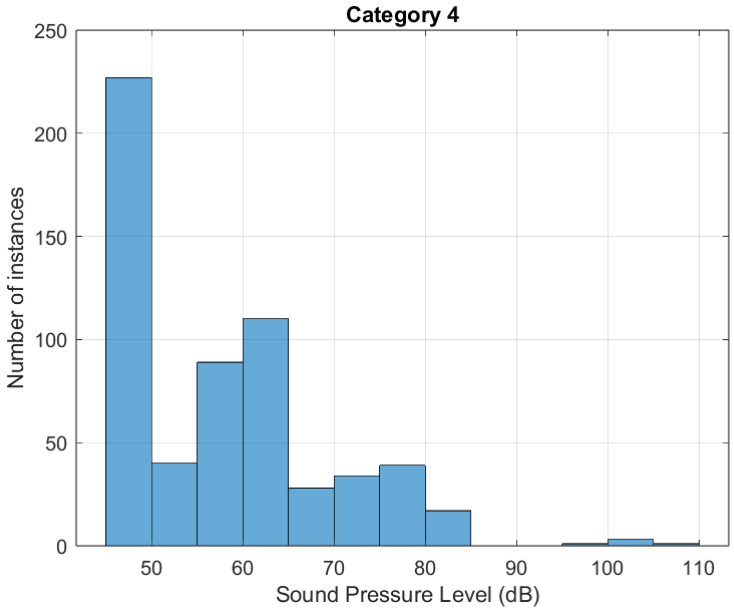

Figure B.4: Distribution of peak sound pressure levels for curve radius category 4.